The University of Manchester

The University of Manchester Research

Geomorphological record of a former ice stream to ice shelf lateral transition zone in Northeast Greenland

DOI:
10.1002/esp.5552

Document Version
Final published version

Link to publication record in Manchester Research Explorer

Citation for published version (APA):
Lane, T. P., Darvill, C. M., Rea, B. R., Bentley, M. J., Smith, J. A., Jamieson, S. S. R., Ócofaigh, C., & Roberts, D. H. (2023). Geomorphological record of a former ice stream to ice shelf lateral transition zone in Northeast Greenland. *Earth Surface Processes and Landforms*. https://doi.org/10.1002/esp.5552

Published in:
Earth Surface Processes and Landforms

Citing this paper
Please note that where the full-text provided on Manchester Research Explorer is the Author Accepted Manuscript or Proof version this may differ from the final Published version. If citing, it is advised that you check and use the publisher's definitive version.

General rights
Copyright and moral rights for the publications made accessible in the Research Explorer are retained by the authors and/or other copyright owners and it is a condition of accessing publications that users recognise and abide by the legal requirements associated with these rights.

Takedown policy
If you believe that this document breaches copyright please refer to the University of Manchester's Takedown Procedures [http://man.ac.uk/04Y6Bo] or contact uml.scholarlycommunications@manchester.ac.uk providing relevant details, so we can investigate your claim.

OPEN ACCESS

Download date:24. Apr. 2024

Geomorphological record of a former ice stream to ice shelf lateral transition zone in Northeast Greenland

Lane, T.P. [1*], Darvill, C.M. [2], Rea, B.R. [3], Bentley, M.J. [4], Smith, J.A. [5], Jamieson, S.S.R. [4], Ó Cofaigh, C. [4], Roberts, D.H. [4]

[1]*Liverpool John Moores University, Liverpool, L3 3AF, UK*
[2]*Department of Geography, The University of Manchester, Oxford Road, Manchester M13 9PL, UK*
[3]*Geography and Environment School of Geosciences, University of Aberdeen, Elphinstone Road, Aberdeen, AB24 3UF, UK*
[4]*Department of Geography, South Road, Durham University, Durham, DH1 3LE UK*
[5]*British Antarctic Survey, High Cross, Madingley Road, Cambridge, CB3 0ET, UK*

*Corresponding Author: t.p.lane@ljmu.ac.uk

ACKNOWLEDGEMENTS

This work was funded through NERC Standard Grant NE/N011228/1. We thank the Alfred Wegner Institute, and particularly Angelika Humbert and Hicham Rafiq, for their logistic support through the iGRIFF project. Further support was provided from Station Nord (Jorgen Skafte), Nordland Air, Air Greenland, and the Joint Arctic Command. Naalakkersuisut, Government of Greenland, provided Scientific Survey (VU-00121) and Export (046/2017) licences for this work. We thank Chris Orton for help with production of figures. Finally, we would like to thank our Field Ranger Isak (after which Isakdalen is informally named) and dog Ooni for keeping us safe in the field. We thank Rob Storrar and an anonymous reviewer for their comments which helped improve the manuscript.

AUTHOR CONTRIBUTIONS

TPL, **CMD**, and **DHR** conceptualised the idea of the manuscript. **DHR**, **BRR**, **MJB**, **SSRJ**, **JAS**, and **COC** acquired funding for the project. **TPL**, **CMD**, **MJB**, **JAS**, **SSRJ** and **DHR** completed fieldwork. **TPL**, **CMD**, **BRR**, and **DHR** completed initial data analysis and wrote the initial draft. All authors assisted with editing the manuscript.

DATA AVAILABILITY STATEMENT

Shapefile data will be stored on the UK Polar Data Centre; https://www.bas.ac.uk/data/uk-pdc/

Article title

Geomorphological record of a former ice stream to ice shelf lateral transition zone in Northeast Greenland

Abstract

Understanding ice stream dynamics over decadal to millennial timescales is crucial for improving numerical model projections of ice sheet behaviour and future ice loss. In marine-terminating settings, ice shelves play a critical role in controlling ice-stream grounding line stability and ice flux to the ocean, but few studies have investigated the terrestrial lateral geomorphological imprint of ice shelves during deglaciation. Here, we document the terrestrial deglacial landsystem of Nioghalvfjerdsfjorden Glacier (79N) in Northeast Greenland, following the Last Glacial Maximum, and the margin's lateral transition to a floating ice shelf. High-elevation areas are influenced by local ice caps and display autochthonous to allochthonous blockfields that mark the interaction of local ice caps with the ice stream below. A thermal transition from cold- to warm-based ice is denoted by the emplacement of erratics onto allochthonous blockfields. Below ~600 m a.s.l. glacially abraded bedrock surfaces and assemblages of lateral moraines, 'hummocky' moraine, fluted terrain, and ice-contact deltas record the former presence of warm-based ice and thinning of the grounded ice stream margin through time. In the outer fjord a range of landforms such as ice shelf moraines, dead-ice topography, and weakly developed ice marginal glaciofluvial outwash was produced by an ice shelf during deglaciation. Along the mid- and inner-fjord areas this ice shelf signal is absent, suggesting ice shelf disintegration prior to grounding line retreat under tidewater conditions. However, below the marine limit, the geomorphological record along the fjord indicates the expansion of the 79N ice shelf during the Neoglacial, which culminated in the Little Ice Age. This was followed by 20th Century recession, with the development of a suite of compressional ice shelf moraines, ice-marginal fluvioglacial corridors, kame terraces, dead-ice terrain, and crevasse infill ridges. These mark rapid ice shelf thinning and typify the present-day ice shelf landsystem in a warming climate.

1. INTRODUCTION

Marine terminating ice streams and their ice shelves are critical components of the global climate system, responding to climate forcings (Goldberg et al., 2009, Gudmundsson, 2013, Reese et al., 2018). Ice shelves buttress ice streams and modulate grounding line dynamics (Scambos et al., 2004). The recent and potential future loss of ice shelves in Greenland and Antarctica could lead to debuttressing of outlet glaciers and ice velocity increases, resulting in rapid ice flux to the oceans and significant sea-level rise (Goldberg et al., 2009, Gudmundsson, 2013, Reese et al., 2018).

Determining the factors that control ice stream and ice shelf stability is important for understanding ice dynamics and for improving models of future ice sheet evolution. Satellite observations have facilitated estimation of grounding line dynamics and rates of ice shelf disintegration over the last 40 years (Hogg et al., 2016, Xie et al., 2018), and sub-ice shelf sediment records from some parts of Antarctica have constrained oscillations over the last 150 years (Smith et al., 2017, Smith et al., 2019). Combined with modern observations, recent and contemporary rates of ice shelf change and grounding line migration are relatively well known. However, longer-term records of ice stream and ice shelf dynamics are required to contextualise modern change.

The offshore geomorphological imprint of ice streams and long-term grounding line retreat is relatively well established (Ó Cofaigh et al., 2002, Batchelor and Dowdeswell, 2015, Dowdeswell et al., 2020), but few studies have investigated the terrestrial geomorphological imprint of topographically constrained ice stream thinning, grounding line retreat and ice stream to ice shelf transition. Of the limited studies executed to date, ice shelf advance and retreat history has been assessed using geomorphologic signals (Sugden and Clapperton, 1981, Roberts et al., 2008, England et al., 1978, England et al., 2009, England et al., 2022) or epishelf lake records (Smith et al., 2006, Roberts et al., 2008, Antoniades et al., 2011, Bentley et al., 2005). In addition, several studies in Antarctica have also attempted to constrain Holocene rates of ice shelf thinning and retreat using surface exposure dating (e.g. Johnson et al., 2014, Mackintosh et al., 2014).

In Greenland, the last ice shelves fronting the Northeast Greenland Ice Stream (NEGIS; Figs. 1 and 2) have started to change dramatically with the disintegration of the Zachariae Isstrøm ice shelf post 2000 CE and rapid thinning of the Nioghalvfjerdsfjorden Glacier (79N) ice shelf due to increased sub-shelf inflow of warm ocean water; (Schaffer et al., 2020) and surface melt (Mayer et al., 2018). The Early Holocene history of NEGIS also suggests the potential for ice shelf disintegration and rapid grounding line retreat (Bennike and Weidick, 2001, Larsen et al., 2018, Bentley et al., 2022, Smith et al., 2022). However, the dynamics of this Holocene lateral transition remain poorly characterised and the geomorphology of ice stream to ice shelf transitions remains largely unconstrained.

This paper aims to investigate the terrestrial landsystem associated with a thinning and retreating ice stream-ice shelf system and develops a geomorphological model for deglaciation, during the Early Holocene, of the Northeast Greenland Ice Stream (NEGIS) and its biggest ice shelf (79N). It examines: (i) the Last Glacial Maximum (LGM) ice stream configuration and interaction between local cold-based ice and the ice stream margin; (ii) the geomorphological signal of ice stream marginal thinning, and (iii) evidence for ice stream to ice shelf lateral transition during both the Early and Late Holocene. Combining this evidence from Northeast Greenland, we present an integrated landsystem model for an ice stream to ice shelf transition zone that can be used to identify such transitional zones and the former presence of ice shelves in the geological record.

2. PREVIOUS WORK

2.1. Geomorphological records of ice streams and ice shelves

The geomorphological imprint of Arctic and Antarctic ice streams and ice shelves has been studied remotely and in the field for several decades. Contemporary ice shelves remain critical, fringing 75% of the Antarctic coastline (Rignot et al., 2013), whereas only a few large ice shelves and ice tongues now remain in the Arctic (Dowdeswell and Jeffries, 2017).

2.1.1. Antarctic

Offshore geomorphology provides the clearest expression of former ice stream expansion and retreat in Antarctica. Geomorphology mapped from high-resolution swath bathymetry has formed the basis of landsystem models used for identifying and interpreting previously unconstrained ice stream and ice shelf dynamics (Andreassen et al., 2014, Graham et al., 2009, Ó Cofaigh et al., 2008).

While investigations of onshore, terrestrial ice stream and ice shelf geomorphology are limited, they have provided theoretical models for understanding ice shelf dynamics. Grounded ice along the margins of George VI Ice Shelf, abutting Alexander Island, created distinctive ice-cored moraines thought to have been formed by thrusting and ablation of debris-rich ice (Sugden and Clapperton, 1981). These landforms combine exotic, far-travelled sediments from the ice stream and reworked local material from the ice margin and sub-ice shelf. Hambrey et al. (2015) invoked 'controlled' moraine formation (Evans,

2009) relating to the structural glaciology of George VI ice shelf, with linear accumulations of ice cored sediment controlled by longitudinal foliation. Subsequently, Davies et al. (2017) found close vertical association of lateral moraines, ice shelf moraines and epishelf lakes (a lake which is impounded in an ice free depression or embayment by an ice shelf or glacier, and is connected to the marine environment (cf. Gibson and Andersen, 2002)), linked with the transition from an ice stream to the George VI Ice Shelf at some point following the LGM. In contrast, on McMurdo Ice Shelf, ice shelf moraines were formed supraglacially, through the release of accreted subglacial sediment entrained into the ice shelf via basal freeze-on of marine waters (Glasser et al., 2006). Fresh water and tidal (epishelf) lakes are also important components of the ice shelf landsystem and sediment records from such lakes have been utilised to constrain reconstructions of ice shelf growth and decay through time (Smith et al., 2006, Roberts et al., 2008, Smith et al., 2007).

2.1.2.Arctic

Many studies have used glacial geomorphology to reconstruct palaeo-ice streams in Canada, Greenland, and Fennoscandia (e.g. Stokes and Clark, 2003, Roberts et al., 2010, Roberts et al., 2013, Lane et al., 2014, Ó Cofaigh et al., 2013, Freire et al., 2015, Newton et al., 2017), and there are limited observations of streamlined bedforms evolving beneath contemporary ice streams (Jakobshavn Isbrae: Jezek et al., 2011, NEGIS: Franke et al., 2020). However, due to the current paucity of Northern Hemisphere ice shelves, few studies have examined Arctic ice stream–ice shelf landsystems (Furze et al., 2018).

Marine evidence suggests that ice streams terminating in floating ice shelves preferentially produce grounding-zone wedges, whereas tidewater margins result in moraine formation (Dowdeswell and Fugelli, 2012, Batchelor and Dowdeswell, 2015). On Ellesmere Island, in the Canadian High Arctic, an abrupt transition of lateral moraines and conical kames to horizontal moraines has been used as evidence of past grounding line position and former presence of an ice shelf (England et al., 1978). The moraines were associated with large, fossiliferous pro-glacial terraces composed of till, ice-rafted debris, and outwash sands, representing a period of ice shelf retreat. Hodgson and Vincent (1984) also reported ice shelf moraines and associated tills deposited up to the marine limit around Viscount Melville Sound in the Canadian High Arctic. Till deposition by the ice shelf was associated with striae and ice marginal fluvial landforms. In the same area, England et al. (2009) noted glaciotectonism of epishelf lake sediments associated with the ice shelf, indicative of marginal glaciofluvial activity. In North Norway, Evans et al. (2002) reported multiple bouldery ice shelf moraines in fjords that contained outlet glaciers during the late glacial, linked to ice shelf migration. In Baffin Bay, offshore swath bathymetry and seismic data revealed large lateral iceshelf moraines, providing evidence for a 500 m thick ice shelf in northern Baffin Bay during the LGM (Couette et al., 2022).

In North Greenland, Larsen et al. (2010) and Möller et al. (2010) described geomorphological evidence for a large, regional ice shelf that flowed east from the Nares Strait along the North Greenland coast. This ice shelf was grounded onshore, depositing a sub-ice shelf till and impounding ice marginal lakes against its southern margin. Glaciolacustrine and glaciofluvial kame sediments deposited above the marine limit record ice shelf presence, prior to deglaciation and the deposition of marine sediments across lower elevations. Preserved dead-ice terrain also suggests burial of the ice shelf margin by marginal glaciofluvial activity during deglaciation. Raised marine deltas at valley mouths up to 40–45 m a.s.l reflect a marine transgression at 10.1 ka following deglaciation (Larsen et al., 2010).

2.2. NEGIS and Nioghalvfjerdsfjorden glacier

NEGIS is the largest ice stream in Greenland, draining ~12% of the ice sheet (Fig. 1; Fahnestock et al., 1993, Joughin et al., 2010). The ice stream branches into three outlet glaciers: Nioghalvfjerdsfjorden Glacier (79N), Zachariae Isstrøm (ZI) and Storstrommen. 79N is the only ice stream with a contemporary buttressing ice shelf. The ZI ice shelf disintegrated after 2010 to leave a grounded tidewater margin. It's retreat and disintegration has been linked to both increased air temperatures and sea ice loss (Khan et al., 2014), and increased submarine melt following the ingress of warm Atlantic water (Mouginot et al., 2015, Schaffer et al., 2020). It is thought that ZI will be highly unstable over the coming decades due to sustained high submarine melt rates and a proximal bed over-deepening (Choi et al., 2017).In contrast, 79N is currently predicted to remain relatively stable for the rest of the century, due to the stabilising effect of ice rises and bedrock island (Choi et al., 2017). The present 79N ice stream and ice shelf are confined to Nioghalvfjerdsfjorden between Kronprins Christian Land to the north and Lambert Land to the south. Higher-elevation terrain is covered in places by local plateau ice caps, mostly on Hovgaard Øer and Lambert Land (Fig. 2).

The geomorphology within Westwind and Norske Troughs (Fig. 1) have been used to reconstruct the former offshore extent of the palaeo-ice stream. Ice stream subglacial landforms such as mega-scale glacial lineations, lateral shear moraines, grounding zone wedges, and De Geer moraines show that the palaeo-ice stream reached the continental shelf break, most likely at the LGM although these landforms are undated (Winkelmann et al., 2010, Arndt et al., 2015, Arndt et al., 2017, Batchelor and Dowdeswell, 2016, Evans et al., 2009). Timing of the initial retreat across the NEGIS outer continental shelf remains uncertain, but occurred between 13.4–12.5 ka BP, driven by an influx of Atlantic Water (Davies et al., 2022). The ice shelf margin then remained close to the inner continental shelf until 11.2–10.8 ka BP, before retreating westwards (Arndt et al., 2017, Davies et al., 2022). Concomitant rates and patterns of ice thinning across the coastal mountains during early deglaciation are unconstrained, despite their importance for numerical model validation. The ice terminus reached the outer coast by ~11.5 ka and retreated to the inner coast by ~10.0–9.0 ka, (Fig. 2, Larsen et al., 2018) This accords with marine biomarker evidence for ice shelf disintegration and NEGIS grounding line retreat to just east of Hovgaard Øer by c. 10.0 ka (west of core site PS100-270VC; Fig. 2; Syring et al., 2020). Evidence for further retreat is constrained by exposure ages of 9.2–7.9 ka west of Blåsø and 9.1–9.0 ka on the south coast of Lambert Land (Fig. 2, Larsen et al., 2018). Radiocarbon dates from Blåsø suggest that the ice shelf retreated between 8.5 and 4.4 ka BP (Smith et al., 2022). This is supported by radiocarbon ages on driftwood and whalebones from palaeo-shorelines which imply open water marine conditions within 79N fjord and Blåsø between 7.0–5.4 cal ka BP (Bennike and Weidick, 2001). This was during the Holocene climatic optimum, an unusually warm period across much of the Arctic from roughly 8.0 to 5.0 ka (Kaufman et al., 2004), which led to extensive ice sheet thinning and retreat (Nielsen et al., 2018).

The location of the NEGIS grounding line between 7.8–1.2 ka is poorly constrained, but Larsen et al. (2018) estimate it was ~20–70 km inland of its present position. The ice shelf is thought to have regrown after 4.4 cal ka BP, coincident with decreasing atmospheric temperatures, and an increase in Polar Water dominance (Smith et al., 2022), reaching its maximum extent during the LIA (Bennike and Weidick, 2001).

3. METHODS

In this study we focussed on the terrain to the north of the 79N outlet (Kronprins Christian Land and Hovgaard Øer; Figs. 2 and 4), and the large island to the south (Lambert Land; Figs. 2 and 5). The locations were chosen for the well-preserved geomorphology, evident from satellite images, and accessibility. The study area was mapped using field and remote mapping. Initial reconnaissance prior to fieldwork was conducted in Google Earth Pro to identify landforms and areas of interest. Where accessible in the field, these areas were targeted for detailed field mapping in 2017, which covered significant regions along the northern side of Nioghalvesfjerdfjorden between Blåsø and Hovgaard Øer. Remote and field mapping were combined to create a geomorphological map (Fig. 4).

Landforms were mapped following Chandler et al. (2018), and the terrestrial landform map was produced using the QGreenland package (Moon et al., 2021) in QGIS 3.22. We identified landforms from Google Earth imagery (dominantly 2017–20 Maxar Technologies) and Landsat satellite imagery—overlain on SRTM and ArcticDEM (vertical accuracy of 2 m and horizontal resolution of 3.8 m). This allowed detailed mapping, and measurement of landform elevations, which are ellipsoidal heights from the ArcticDEM (roughly 30 m above geoidal heights). Ice shelf geomorphology mapping was undertaken separately in Esri ArcMap using ArcticDEM and Google Earth Pro. Ice surface velocity data was obtained from the MEaSUREs Greenland Ice Sheet Velocity Map and sub-shelf bathymetry and subglacial topography was taken from BedMachine v3 (Morlighem et al., 2017). Ice surface reconstructions were plotted using a 1° surface slope in line with the current ice sheet surface in this region.

4. RESULTS

4.1. ***Local glaciation***

Local ice occurs at higher elevations to the west of the study area (>800 m a.s.l.) and lower elevations closer to the coast in the east (>500 m a.s.l.). Some plateau ice cap outlet glaciers extend down to sea level. The geomorphological imprint of local ice masses at higher elevations is limited, as past expansion has caused little erosion or deposition and evidence of meltwater drainage forming ice marginal channels is rare. Where outlets reached lower elevations (e.g., Hovgaard Øer) they formed arcuate, latero-terminal moraines, distinguishable from landforms formed by the ice shelf margin based on their orientation and morphology.

4.2. Blockfields

Autochthonous blockfields are common at elevations above ~900 m a.s.l. On Hovgaard Øer they extend continuously over hundreds of vertical metres and consist of clast-supported, angular to very angular blocks of local quartzite bedrock with no erratics (Fig. 3A and 3B). Most boulders are less than a metre (a-axis), with some larger exceptions reaching up to three metres (a-axis). The autochthonous blockfields transition downslope to matrix-supported allochthonous blockfields between 900–600 m a.s.l. and contain both local quartzite and far-travelled erratics (sandstone, limestone, conglomerate: Figs.

3C and 3D). The allochthonous blockfields can be traced away from plateau summits, draping the landscape downslope with signs of movement via gelifluction. Indeed, evidence for periglacial processes is widespread in the form of patterned ground, debris stripes and gelifluction lobes. These high-elevation, autochthonous blockfields above ~900 m a.s.l. are interpreted as *in situ* regolith, indicating little or no glacial erosion over extended time periods (10–100's ka; Rea et al., 1996, Ballantyne, 2018).

Between ~600–0 m a.s.l. along the northern margins of 79N fjord, the terrain continues to be dominated by allochthonous blockfields and sediments reworked by slope processes, but with a noticeably higher quantity of glacially-abraded erratics. The landscape at this elevation is interspersed with localised (<1 km^2) outcrops of glacially abraded bedrock, typically below 200 m a.s.l on promontories projecting into the fjord (e.g., southern coast of Hovgaard Øer), displaying striations and perched erratic boulders. The presence of erratic boulders on allochthonous blockfield slopes between 900–600 m a.s.l. is clear evidence for past ice cover.

4.3. Ice stream geomorphology

4.3.1. Moraine ridges

Moraines are common between 600–200 m a.s.l. along the northern side of 79N fjord (Fig. 4), and the southern edge of Lambert Land (Fig. 5). They are characterised by distinctive arcuate lateral ridges (Figs. 6A and 6B) and 'hummocky' moraine complexes (Figs. 6C and 6D). In some cases, moraines are nested, often linked to raised deltas (Fig. 7). One of the clearest examples of an arcuate, single-crested moraine runs roughly NW–SE, skirting a broad valley for over 6 km at 600–580m a.s.l. (79.692°N, 21.476°W), (Figs. 4A, 4B, 6A and 6B). The ridge is more than 10 m high and consists of unconsolidated diamict ranging from silt to boulders of varying lithologies. Occasional boulders up to a metre in diameter were observed. Nested lateral moraines occur within marginal valleys and cols adjacent to the 79N fjord, most commonly between 450–300 m a.s.l. but also evident down to ~200 m a.s.l. The clearest examples are found on both the northern and southern sides of Isakdalen (informal name) — northeast of Blåsø — from 430–320 m a.s.l. (Fig. 4A). These moraines are 5–8 m high, up to 20 m wide, and composed of mixed lithologies of unconsolidated diamict. Ridge crests are often sub-horizontal where intact, but many are heavily degraded downslope by periglacial activity. Together these are interpreted as lateral or terminal moraine, recording previous ice sheet extent (Benn and Evans, 2014).

In some locations arcuate moraine ridges fragment into zones of distinctive 'hummocky' moraine. These zones comprise broad chains of linear to conical ridges composed of partially sorted sediment and interspersed with kettle holes (Figs. 6C, and 6D). Occasionally they have flat upper surfaces. The best examples of these are found in the east of Isakdalen (Fig. 4A), at an interfluve between Isakdalen and the 79N fjord. In cross profile, conical moraines have steep proximal and distal sides with high angles of repose (Figs. 6C, and 6D). These are interpreted as 'hummocky' moraine, formed through ice-stagnation (Benn and Evans, 2014, Benn, 1992).

4.3.2. Deltas

Perched deltas occur between 520–55 m a.s.l. on the northern 79N fjord wall, the south of Hovgaard Øer (Fig. 4A) and Lambert Land (Fig. 5A). There are isolated examples, but they commonly occur in sets of altitudinally-zoned "staircases" within marginal valleys. Many appear pristine, with smooth, gently grading tops, sharply defined ice-proximal slopes, and well-preserved lateral drainage channels (Fig. 7). The deltas are composed of well-sorted glaciofluvial sediments from silts, through sands, to cobbles. Some have been fragmented due to periglacial disturbance including the development of ice wedge polygons.

Large deltas are particularly prevalent in a discontinuous, NW–SE staircase on the floor of Isakdalen, leading down to the northern side of the 79N fjord (Fig. 4A). The highest of these deltas is at ~300 m a.s.l and closely associated with 'hummocky' moraine at 79.645°N, 21.785°W. The staircase is long (5.5 km) and narrow (0.7 km) and can be traced downslope, towards the southeast to ~50 m a.s.l (Fig. 4A). Further east, another delta complex is associated with streamlined, fluted glacial sediment that extends down-slope of the delta and a former ice margin denoted by a clear drift limit. Their geomorphology and location suggests they are deltas, formed in either a glacier-fed or ice-contact setting (Benn and Evans, 2014).

4.3.3. Channels

Bedrock- and sediment-incised channels run across valley slopes and most commonly sub-parallel to lateral moraines. Bedrock-incised channels are short (<1 km) and steep, and relatively deep (approximately 50–10 m), and occasionally cut across local watersheds. These appear to be overspill channels, formed through water overspill and incision following ice damming (Lane et al., 2015a). In contrast, channels that run sub-parallel to lateral moraine ridges are generally shallower with lower gradients and are often nested. In some cases, they occur at the transition between lateral and 'hummocky' moraine, such as at Isakdalen (Fig. 4) and on the southwestern slopes of Lambert Land (Fig. 5). These are interpreted as lateral meltwater channels (Kleman et al., 1997).

4.3.4. Streamlined terrain

Allochthonous blockfields drape the landscape adjacent to the northern edge of the 79N fjord at 900–600 m a.s.l. Bedrock outcrops appear between 600–400 m a.s.l., showing some limited evidence of smoothing and striations although surfaces are not heavily abraded. Below 400 m a.s.l., bedrock is heavily abraded and scoured along the fjord walls (Fig. 8), particularly towards the east on the lower, south-facing flanks of Hovgaard Øer. Here, gneissic bedrock has been abraded and plucked to form whalebacks and roches moutonnées (Fig. 8B). Striae are orientated west-east, and plucked faces are found on the east side of roches moutonnées, consistent with eastwards ice flow. There are erratic boulders of mixed lithology (e.g., quartz, quartzite, conglomerate, sandstone, limestone) scattered across the surface of scoured bedrock. Abraded bedrock outcrops with frequent perched boulders were also found further up-fjord, at the western end of Blåsø, from 600–100 m a.s.l.

4.4. Ice shelf geomorphology

4.4.1. Ice-marginal linear ridges

A complex of nested, linear ridges runs intermittently for over 40 km sub-parallel to the northwest margin of the 79N ice shelf (Fig. 9). These are all at low elevation (<30m a.s.l.) with the largest, outer ridges sharply-defined, 5–10 m high and up to 10 m wide. Inboard of the larger ridges are a series of smaller linear ridges <5 m in height and width, forming an inset sequence of up to approximately 20 ridges between the outer limit and the present ice shelf margin. Active fluvial channels and lakes occur on the distal side of the ridges (Fig. 9B) and, where the ridges are breached, small fan systems have formed. On the ice proximal side of the ridges, a band of debris-covered ice up to a few hundred metres wide forms actively down-wasting terrain within which the sediment is being reworked by glaciofluvial processes (Figs. 9A and 9B). To the west of Blåsø, exposures within outer linear ridges were found to be composed of reworked and folded marine shell-bearing muds. These linear ridges formed asymmetrically stacked sequences of deformed sediment emplaced over exposed bedrock.

On the southern coast of Hovgaard Øer, a series of degraded lateral moraines and ice-marginal lakes occur at ~400–60 m a.s.l. (Fig. 10). At ~65 m a.s.l. (the local marine limit) a distinctive, grey-coloured glacial drift forms a lobate margin composed of a series of fragmented flat surfaces containing distinctive kettle holes. Overprinting this terrain is a second lobate margin composed of pink-coloured drift running adjacent to the coast at ~10 m a.s.l. The pink-coloured sediments are also heavily degraded but have fragmented linear ridges running west–east that lie sub-parallel to the coast.

4.4.2. Transverse ridges

Transverse ridges running obliquely into the ice-marginal linear ridges are ubiquitous in the mid-fjord area, adjacent to the current northern edge of the ice shelf margin (Figs. 9A). These landforms vary from arcuate to straight in planform but can be partially sinuous and crenulated in short sections. Sub-sets of ridges also run at opposing oblique angles to one another. In many localities they mimic the tensional crevasse patterns observed on the adjacent ice shelf.

4.4.3.Ice-marginal and epishelf lakes

Many of the larger ice-marginal linear ridges impound small lakes adjacent to high ground. The lakes are generally linear or ovate in planform (Fig. 9B and C), often forming a series of ribbon lakes. Multiple shorelines associated with these lakes record fluctuating water levels and perched lake sediment sequences were observed to contain laminated silts and muds with occasional dropstones. Some small lakes are impounded directly between the debris-free ice-shelf edge and the steep sides of the 79N fjord. In places, lakes have drained via overspill channels. Epishelf lakes, which have a direct connection to marine water under the ice shelf, are likely found along the edge of the ice shelf, but only in Blåsø is there direct observational evidence of a tidal marine influence (Bentley et al., 2022).

4.4.4.Present-day ice shelf-marginal channels

Glaciofluvial sediments are common along the ice shelf margin. Corridors of channelised glaciofluvial sediments are clearly observed along the northern side of 79N with some channels being highly sinuous and mirroring supraglacial channels on the adjacent ice-shelf surface (Fig. 9B). Elsewhere, channel systems are shallow and braided adjacent to the ice-shelf margin and beyond the LIA maximum limit. Sedimentation associated with these channels has partially buried the ice shelf margin in many places, resulting in fragmented, ice stagnation topography, with the development of kame and kettle topography, and sub-horizontal outwash surfaces interspersed with chaotic, dead-ice terrain (Fig. 9B). A number of sinuous ridges may also be engorged eskers.

4.5. Ice shelf structural glaciology

The north-western (NW) and south-eastern (SE) margins of the ice shelf contrast in terms of morphology and flow characteristics. Along the NW margin there are three unconstrained ice flow outlets from the ice shelf, one into each of the western and eastern ends of Blåsø, and one north into Dijmphna Sund (Fig. 2). There are no inflowing glaciers downstream of the grounding line. In contrast, along the SE margin multiple ice field glaciers flow into the ice stream from Lambert Land, creating prominent flow units and there are no outlets. The front of the ice shelf abuts the small islands of Bloch Nunnatakker.

The contemporary ice shelf has several distinctive structural elements that provide insights into the geomorphological signal observed along the ice shelf margin. The ice shelf stretches a little over 70 km from the present grounding line and is, in places, greater than 20 km wide (Mouginot et al., 2015). The dominant features of the shelf are longitudinal, approximately flow-parallel features, which appear to be initiated proximal to the grounding line (Fig. 9a). Given the presence of substantial annual surface melt, these features appear to be enhanced by channelling surface meltwater.

The ice which flows into the western side of Blåsø is sourced entirely from relatively slow moving (<100 ma^{-1}) grounded ice and appears to be partially grounded as it enters the epishelf lake (Bentley et al., 2022). "Midgardsormen", which has been associated with compression in the ice shelf as it flowed obliquely across a lateral grounding line was described by (2018). It is no longer visible at the western entrance to Blåsø, suggesting the ice shelf no longer grounds in this manner at that location. Multiple Midgardsormen ridges can be seen along much of the rest of the NW margin, eastwards to Dijmphna Sund (Figs. 9a and 9b) and as the ice shelf impinges on the southern shore of Hovgaard Øer.. They are generally confined to within about 1 km inboard from, and are oriented sub-parallel to, the ice shelf lateral margin, but in a few locations, they angle obliquely towards the ice shelf. For the most part these appear in regions of the ice shelf calculated to be close to the floating-grounded marginal transition, by subtracting the elevation of the ice shelf base (assuming it is in hydrostatic equilibrium) from the bathymetry taken from Bed Machine v3 (Bentley et al., 2022). Other similar lateral ridges are observed

5. DISCUSSION

5.1. Evidence for local cold-based ice

The landscape we report surrounding 79N is typical of pan-North Atlantic glaciated continental margins. Substantial selective linear erosion by marine terminating ice streams results in deeply incised fjords separated by high elevation relict plateaux surfaces (Sugden, 1974, Roberts et al., 2013, Lane et al., 2016, Kessler et al., 2008). Such plateaux host modern ice caps that are cold-based and—given the absence of significant erosional landforms or meltwater features on the plateaux—have likely experienced cold-based ice cover throughout much of the Quaternary, either from expanded local ice caps, or cold-based portions of the Greenland ice sheet. This difference in thermal regime is supported by inherited cosmogenic isotope signals on such Greenlandic plateau surfaces (Strunk et al., 2017, Briner et al., 2014). Elsewhere in Greenland, ice drawdown by ice streams in landscapes of selective linear erosion has been invoked as a means of starving peripheral high elevation plateaux of erosive ice (Roberts et al., 2013, Lane et al., 2016, Beel et al., 2016).

The high-elevation autochthonous blockfields are likely to have remained ice-free for much of the Quaternary and/or been periodically covered by thin, non-erosive ice (Strunk et al., 2017). Dual $^{10}Be/^{26}Al$ nuclide concentrations from bedrock and erratic samples at 900–500 m a.s.l. in Dove Bugt — south of the study area — highlight slow rates of plateau erosion since 0.6–1.0 Ma, although it is unclear for what percentage of time autochthonous blockfields have been buried or exposed (Skov et al., 2020). It is also hypothesised that the slow erosion rates post 0.6 Ma mark the onset of accelerated ice sheet incision resulting in the development of overdeepened fjords, and the abandonment of ice sheet erosion of high-level surfaces (Skov et al., 2020).

Allochthonous blockfields are extensive between 900 and 600 m a.s.l., and provide clear evidence of past ice cover suggesting erratics were transported and deposited by cold-based ice that preserved the underlying periglacial landscape. Allochthonous blockfields can also form from old glacial material (Dahl, 1966), meaning it is possible that these areas developed slowly, from a Late Pliocene to Mid Pleistocene till cover, supporting the hypothesis of long-term fjord development highlighted by Skov et al. (2020).

Passive emplacement of erratics on blockfields is likely linked to a transition from warm- to cold-based ice within the 79N ice stream up flow from the site during the LGM (cf. Sugden and Watts, 1977, Roberts et al., 2013, Rea et al., 1998). Indeed, erratics from summit areas on Store Koldeway and Pusterdal (south of our study area) also show emplacement by ice across high elevation plateau terrain during the last glacial cycle (Skov et al., 2020). Furthermore, there is clear evidence of an elevationally-controlled transition to enhanced warm-based subglacial erosion below 460 m a.s.l. in the landscape around Dove Bugt. This finding accords with our own interpretation reported above highlighting enhanced subglacial erosion below 600 m a.s.l. and the development of scoured and abraded bedrock surfaces.

In general, there is limited evidence for moraines formed by local ice masses at high elevation. Only where local ice caps expanded and transitioned to polythermal outlet glaciers are moraines found at low elevations in the landscape. Hence, there is definitive evidence to support local ice cap fluctuation and expansion, which infers localised areas of blockfields have remained intact and undisturbed despite being overrun during the Holocene. Questions pertaining to the burial or long-term exposure of blockfields (Skov et al., 2020) can be hypothetically investigated using the Holocene record.

5.2. Deglaciation and ice stream thinning

An assemblage of distinctive glacial landforms indicates the maximum thickness of the 79N ice stream during the LGM and subsequent thinning during deglaciation. From highest to lowest elevation, these features are streamlined bedrock terrain, lateral moraines, 'hummocky' moraine, and perched deltas. This landform assemblage is found in various locations in the study area, most prominently as vertical staircases on the slopes and marginal valleys on the northern side of the 79N fjord (see Fig. 13).

5.2.1.Streamlined bedrock terrain

Below the zone of allochthonous blockfields between 900–600 m a.s.l. striae and plucked bedrock surfaces (Figs. 2 and 7a) confirm a thermal transition to warm-based ice flowing eastwards along the fjord. Areas of scoured bedrock are covered by patchy glacial sediment and a mixed assemblage of erratics which indicate ice flow sourced from the west (Pedersen et al., 2013). Sculpting and abrasion to form crude bedrock bedforms and roches moutonnées are typical of hard-bed processes dominated by basal sliding and commonly associated with areas of areal scour and ice streaming beneath outlet glaciers/isbræ from the Greenland Ice Sheet (e.g. Roberts and Long, 2005, Lane et al., 2015b, Skov et al., 2020). Less frequently reported in terrestrial settings in Greenland is evidence for subglacial sediment deformation (Lea et al., 2014, Pearce et al., 2018). Areas of streamlined drift and flutes adjacent to the northern 79N margin demonstrate ice was not only warm-based but operating over a deforming bed in places. Such conditions are common in submarginal locations associated with ice streams, with deforming bed tills playing a pivotal role in controlling ice stream dynamics and marginal stability (Roberson et al., 2011, Ó Cofaigh et al., 2002, Ó Cofaigh et al., 2007).

5.2.2.Lateral moraines

Distinctive arcuate moraine ridges on the northern side of the 79N fjord mark the limits of a thicker NEGIS which flowed north and eastwards across the high elevation landscape (Fig. 11). Allochthonous blockfields occur above the moraines, highlighting the likely transition from cold- to warm-based ice. The highest elevation ridges at ~600 m a.s.l. record a minimum ice thickness of 1500 m within the trough. Many of these moraines skirt valley edges and topographic depressions, suggesting partially constrained ice. This juxtaposition of cold- and warm-based ice along a palaeo-ice stream margin has been noted elsewhere in Greenland (Skov et al., 2020, Roberts et al., 2013). For example, the

Uummannaq ice stream produced similar high-elevation lateral moraines demonstrating that ice overtopped steep confining fjord walls and locally pushed onto, high elevation plateaux areas above ~750–800 m a.s.l. (Lane et al., 2014, Roberts et al., 2013). As the 79N ice stream thinned, it gradually withdrew from the higher elevation landscape, depositing sequences of nested lateral moraine ridges north of 79N (Fig. 11) and on Lambert Land (Fig. 12), demonstrating periodic ice stream stabilisation during overall deglaciation. This is similar to other ice stream marginal settings where thinning produces staircases of nested lateral moraines in fjord settings (Davies et al., 2017).

Zones of distinctive 'hummocky' moraine occur in places below arcuate moraine ridges, most notably at ~350–410 m a.s.l. in eastern Isakdalen (Figs. 4 and 11). We attribute these features to ice contact/marginal deposition during ice stagnation. The steep proximal sides of the conical hummocks, partially sorted sediment and kettle holes are indicative of glaciofluvial fans or kames deposited in coalescent ice marginal settings where meltwater is routed between ice masses and where the subsequent secondary deposition of fluvioglacial sediment begins to partially bury the ice margin. In Isakdalen, the topographic position of the hummocks demonstrate that they formed in a zone of coalescence between two retreating ice masses, with ice receding both to the northwest into Isakdalen and southwards towards 79N (see centre of Figs. 11D–F). Such suture zones provided conduits for the routing of meltwater, but also ice marginal environments within which water became ponded. The flat-topped surfaces of a number of hummocks further suggests ponding and ice-walled conditions in these coalescent zones (cf. Evans et al., 2017).

5.2.3.Deltas

Large glacio-lacustrine deltas are particularly prominent at ~300–50 m a.s.l. in Isakdalen, and the valley to the north (Figs. 4 and 11), with smaller equivalents found at ~60 m a.s.l. on Hovgaard Øer (Figs. 5 and 12). These all exist above the marine limit, as reported by Bennike and Weidick (2001). We infer delta staircases record meltwater ponding at progressively lower elevations as the ice stream thinned during deglaciation (Figs. 11D–F). The presence of ice dammed lakes indicates significant meltwater production and a quasi-stable terrestrial ice margin. Additionally, the evidence of a fluted, deforming bed associated with these ice margins supports the presence of warm-based active ice along the ice stream margin during deglaciation. Hence, delta staircases appear to record gradual lowering of the ice stream surface and emergence of the fjord walls during deglaciation.

5.2.4. Ice stream landsystem summary

This landform assemblage (summarised in Fig. 13A) resembles systems reported in northern Canada and Greenland where former grounded ice margins occurred above the local marine limit (England et al., 1978, Larsen et al., 2010, Möller et al., 2010). The perched deltas along the 79N fjord are particularly important geomorphological constraints on ice stream thinning and concomitant retreat of the grounding line from the outer coast to the inner fjord. Deglaciation of 79N from the outer coast to the inner fjord is presently constrained to 10.2–7.9 ka (Bennike and Weidick, 2001, Larsen et al., 2018) but these age constraints are from low elevation sites and do not capture evidence for antecedent thinning which may have conditioned a rapid grounding line retreat and ice shelf disintegration. The delta sequences record the emergence of the coastal mountains and fjord prior to 10.2 ka. The association of chains of 'hummocky' moraine composed of sorted sediment with arcuate moraines and deltas suggest the formation of kames and deltas as marginal meltwater began to flow and pond along the ice margin. Increased meltwater production implicates atmospheric warming as at least a partial driver of the deglaciation.

The delta staircases can be traced down to ~50m a.s.l in Isakdalen and ~65m a.s.l on Hovgaard Øer just above the local marine limit (Bennike and Weidick, 2001), tracking the thinning of a grounded ice margin until full deglaciation, after which sea-level began to fall (Bennike and Weidick, 2001). There is little evidence for a transition to an ice shelf from the mid to inner-fjord during deglaciation, suggesting that the 79N ice stream may have remained grounded but was not fronted by an accompanying ice shelf as it passed through mid- to inner- fjord (Smith et al., 2022, Bennike and Weidick, 2001).

5.3. Ice stream–ice shelf transition

5.3.1. An Early Holocene ice shelf retreat signal in Nioghalvesfjerdfjorden?

There is a clear geomorphological distinction between the terrestrial landforms generated during deglaciation by the grounded ice stream margin and landforms produced during a subsequent ice shelf (floating ice) expansion in the late Holocene (Bennike and Weidick, 2001, Smith et al., 2022). The regional marine limit ranges from ~70–65 m a.s.l in the east to 40–35 m a.s.l in the west adjacent to Blåsø (Bennike and Weidick, 2001). The assemblage of lateral moraines, 'hummocky' moraine and staircases of perched deltas are found above this and records the thinning of the grounded ice stream margin (Figs. 4, 6, and 7).

On Hovgaard Øer an upper ice shelf limit is marked by a moraine composed of grey glacial sediment (Fig. 10). This hypothesised ice shelf limit is coincident with the marine limit at ~65 m a.s.l. *Portlandia arctica* molluscs from the ice shelf moraine sediment have been dated to 9.8–9.5 cal. ka (Bennike and Weidick, 2001), confirming that this represents a deglacial phase ice shelf margin. Several key landforms including kettle holes, linear moraine ridges, ice marginal channels and kame terraces, and small ice marginal lakes mirror the geomorphological signal of the post-LIA ice shelf landsystem identified below. This ice shelf limit has been heavily degraded by periglacial activity, possibly confirming the antiquity of this particular area of Hovgaard Øer. Overprinting this Early Holocene ice shelf limit is a suite of landforms that relate to the later LIA ice shelf re-expansion.

The timing of ice retreat and thinning through 79N fjord can be bracketed by offshore and onshore deglacial ages. Deglaciation from the outer continental shelf was in progress by 15 ka (Stein et al., 1996), coincident with upstream ice sheet thinning along the fjord and emergence of the coastal mountains. Ice stream thinning would have been antecedent-to-concomitant with grounding line retreat, which reached the outer coast and fjord mouth by ~11.5–8.9 ka (Larsen et al., 2018). Ice subsequently began retreating through 79N fjord ~10.2–7.9 ka (Larsen et al., 2018). Despite the localised evidence for an ice shelf on Hovgaard Øer at the opening of the Holocene, there is no confirmatory evidence of such an ice shelf in mid- or inner-fjord locations. The implication may be rapid grounding line retreat under tidewater conditions through Nioghalvesfjerdfjorden i.e., rapid retreat is suggestive that there was no substantive ice shelf which would likely have supported a slower retreat. This hypothesis accords with Syring et al. (2020) who reported ice shelf disintegration prior to grounding line retreat inboard of the pinning point at the mouth of Nioghalvesfjerdfjorden at ~10.0–9.0 ka. It is further corroborated by evidence of open marine conditions in Blåsø by 8.5 ka (Bennike and Weidick, 2001, Larsen et al., 2018, Smith et al., 2022). The rapid breakup of an ice shelf during deglaciation has been reported in other High Arctic locations, with England et al. (2022) recording the catastrophic collapse of the Viscount Melville Sound ice shelf along the north-western Laurentide Ice Sheet, with ice shelf advance collapse occurring in 150 yrs.

5.3.2.Neoglacial ice shelf regrowth

Along the northern margins of 79N the ice shelf landsystem has several distinct elements. Firstly, large, sharp-crested linear moraine ridges are often composed of bulldozed and folded sediments suggesting many are ice shelf push moraines. Inboard of the outer linear moraine ridges are a series of smaller, ice flow parallel linear ridges (Fig. 9). They are interpreted to represent compression, folding and foliation development along the margin of the ice shelf. They may originate from lateral compression of the ice stream proximal to the grounding line as it transitioned to a floating ice shelf or alternatively, they may be a product of localised lateral compression of the ice shelf margin. Folding related to either process may bring subglacial debris to the ice surface (Fig. 13) and these may be a form of 'controlled' moraine (Evans, 2009, Hambrey et al., 2015). A further structural influence exerted by the ice shelf margin is manifest in the short, sinuous, and crenulated ridges that sit inboard of the ice shelf moraines. These are interpreted as remnants of crevasse infills (Evans et al., 2016) formed through the interaction of ice marginal or supraglacial streams with the ice shelf margin.

Given the position of the outermost, large linear moraine ridges, close to the current ice shelf margin (see Fig. 9b), they are taken to mark the limit of 79N ice shelf during the LIA. Bennike and Weidick (2001) sampled reworked marine shells within these ridges which dated to the early Neoglacial, marking ice shelf re-expansion during the Mid- to Late-Holocene. This is supported by evidence from sediment cores in Blåsø which record ice shelf regrowth after 4.4 cal ka BP reaching its present thickness by 4.0 cal ka BP.

Depending on the ice shelf margin geometry and marginal fjord bathymetry, marginal lakes may be fully marine, epishelf, or transitional and are commonly associated with ice shelves in the Arctic (England et al., 1978, England et al., 2009, Hodgson and Vincent, 1984, Larsen et al., 2010, Möller et al., 2010) and Antarctic (Hambrey et al., 2015). We found no evidence of large-scale deltas forming in these lakes compared to the ice stream marginal landsystem outlined above—likely due to shallower water depths (fans are evident) and much smaller catchments with concomitant reduction in water and sediment supply. The lakes act as local sedimentary depo-centres and together with the fluvioglacial corridors that form kame terraces lead to the development of a confined linear ice marginal landsystem similar to those reported from other ice shelf marginal settings in the Canadian High Arctic (Hodgson and Vincent, 1984, England et al., 2009). Importantly once the outer linear moraine ridges are breached, the glaciofluvial transport of sediment leads to the partial burial of the ice shelf margin and the potential for longer-term development of distinctive dead ice topography.

The ice shelf geomorphological signal that occurs below the marine limit records the advance of an ice shelf in the Late Holocene, likely starting in the Older Neoglacial and culminating in the LIA (Briner et al., 2016). Minimum ice extent in the early Holocene remains unknown. Larsen et al. (2018) speculated that the NEGIS grounding line was 20–70 km up-ice of the present-day grounding line between 7.8–1.2 ka, but Smith et al. (2022) record the ice shelf reforming at Blåsø by c. 4.4 cal ka BP. This is supported by earlier estimates of ice shelf re-growth as indicated by driftwood and whale bone from c. 5.4 ka cal BP (Bennike and Weidick, 2001).

Following the LIA, ice shelves fronting NEGIS have thinned, retreated and disintegrated. Over the last two decades the ZI ice shelf disintegrated after 2010 and the 79N ice shelf has thinned by 30% between 1999 to 2014 (Mayer et al., 2018). The rapid thinning of the 79N ice shelf has resulted in the ice shelf marginal landform signal reported here (see Figs. 9 and 13b). Its preservation potential is likely to be poor and ultimately dependent on the thickness of the ice shelf margin, structural glaciological controls, fjord wall geometry, the rate of buried dead-ice decay, sea level vs isostatic rebound and reworking by secondary processes. Notably, geomorphological evidence of ice shelf thinning during deglaciation is sparse, because deglacial dates suggest the ice shelf collapsed leading to rapid grounding line retreat through the mid- to inner-79N fjord (Smith et al., 2022). In its present guise the rapidly evolving margin of the 79N ice shelf typifies the geomorphological signal of an ice shelf marginal landsystem in a rapidly warming climate where the rate of ice shelf thinning, rather than rapid ice margin retreat, is the key control on its morphostratigraphic signal, though this may rapidly change if the ice shelf starts to collapse.

6. CONCLUSIONS

Our study shows that the geomorphological imprint of Nioghalvfjerdsfjorden Glacier records a lateral transition from a grounded ice stream to a floating ice shelf during deglaciation. Above 900 m a.s.l., terrain is covered by local ice caps or autochthonous blockfields. From 900–600 m a.s.l., autochthonous blockfields transition to allochthonous blockfields with local and far-travelled erratics, recording the lateral transition from cold- to warm-based and faster flowing ice within the fjord. Below 600 m a.s.l., lateral and 'hummocky' moraines, ice-contact deltas, and abraded bedrock provide evidence for a warm-based, grounded ice stream with a thinning margin. Landform evidence in the outer fjord at Hovgaard Øer records the presence of an ice shelf moraine, deposited during deglaciation. This geomorphological signal is absent along the rest of the fjord, suggesting ice shelf breakup prior to—or during—the onset of ice stream retreat through the fjord.

The 79N ice shelf expanded during the Neoglacial, reaching a maximum at the LIA, and subsequently thinned during the latter part of the 20th Century with acceleration of the thinning during the 21st Century. This has resulted in a suite of ice shelf moraines formed through marginal bulldozing with secondary controlled-moraine development, ice marginal epishelf and freshwater lakes, kame terraces and ice stagnation topography produced through ice marginal fluvioglacial corridor development and sediment burial. Collectively, these record the geomorphological signal of a rapidly thinning ice shelf in a warming climate.

Figure 1. Overview of Northeast Greenland, showing the NEGIS drainage basin (black solid line) and ice sheet velocity, generated using auto-RIFT (Gardner et al., 2018) and provided by the NASA MEaSUREs ITS_LIVE project (Gardner et al., 2019). Overlain on the ArcticDEM with IBCAO bathymetry (Jakobsson et al., 2020). Black dashed box shows location of Fig. 2. Figure generated using QGreenland (Moon et al., 2021).

Figure 2. Map of the NEGIS region (A) localities mentioned in the text overlain on Sentinel-2 imagery (courtesy of the U.S. Geological Survey). The location of marine core PS100-270VC (red circle), surface exposure ages (yellow circles, from Larsen et al. 2018), and radiocarbon ages (white circle, from Smith et al. 2022) are shown. X-X' are the location of the profile in Fig. 13. (B) Digital elevation model of the region, with terrain above 900 m a.s.l. and 600-900 m a.s.l. shaded. These areas are broadly coincident with autochthonous and allochthonous blockfields respectively (Fig. 3).

Figure 3. Blockfields on Hovgaard Øer. (A and B) Autochthonous blockfield at ~1000 m a.s.l. (C and D) Lower elevation (~650 m a.s.l.) allochthonous blockfield with common orange-brown sandstone erratics. Black box in C shows the location of A and B. (E) Local ice mass on Hovgaard Øer with clear arcuate latero-terminal moraines. (F) Oblique aerial photograph of the allochthonous blockfield east of Blåsø, showing clear debris stripes and evidence for gelifluction.

Figure 4. Glacial geomorphology northeast of Blåsø (location shown on Fig. 2). (A) Geomorphological map of the northern 79N region; (B) high elevation (~600 m a.s.l.) latero-terminal moraine; (C) lateral moraine which continues from Blåsø to Isakdalen; (D) one of the delta staircases. Arrows in B and C indicate inferred palaeoice flow direction. Mapping overlain on ArcticDEM, generated using QGreenland (Moon et al., 2021). White arrows in B and C indicate the location of the moraine ridges.

Figure 5. (A) Glacial geomorphology of the southwest coast of Lambert Land (location shown on Fig. 2). Contemporary 79N ice is shown by white shading. Black lines denote lateral moraine staircases, yellow polygons mark individual deltas and delta staircases. There are also ice marginal channels (yellow lines) which often run sub-parallel to lateral moraines. (B and C) Satellite images showing examples of ice marginal channels found in the study area.

Figure 6. (A) Oblique aerial and (B) crest-top photographs of the highest elevation ice stream moraine mapped in the study (Box B in Fig. 4A). (C, D) Oblique aerial photographs of 'hummocky' terrain showing conical mounds and circular pools, located at the eastern end of Isakdalen (see Fig. 4a for location).

Figure 7. (A and B) Oblique aerial and (C) ground-level photographs of a delta staircases (see Figs. 4a and 4d for location). Photograph C is taken from the lowest delta surface seen in panel A.

Figure 8. Photographs of glacially abraded bedrock surfaces on the south of Hovgaard Øer. A thin, layer of coarse till is visible between areas of exposed bedrock, along with common glacially transported erratics. Striae direction is shown by the black arrow in A.

Figure 9. (A) overview of the northern margin 79N ice shelf. (B) Oblique aerial photograph showing ice shelf geomorphology mid 79N fjord. Note: 1) Midgardsommen ridge; 2) linear and ovate supraglacial drainage controlled by longitudinal foliation in the ice shelf; 3) burial of ice shelf margin by fluvioglacial sediment/development of ice stagnation topography and localised ponding; 4) linear ridges; 5) outwash fans; 6) braided fluvioglacial corridors forming kame terraces. (C) Oblique aerial photograph showing ice shelf geomorphology west of Blåsø. Note: 7) longitudinal foliation exposed in section along the grounded ice shelf margin; 8) braided outwash surfaces; 9) crevasses infills; 10) supraglacial fluvial corridor; 11) the Little Ice Age shelf moraine impounding marginal lakes

Fig. 10. (A) Photograph looking over the southern coast of Hovgaard Øer, showing pink and grey drift, and kettle holes. Photo location shown in B. (B) Glacial geomorphology from the south coast of Hovgaard Øer, overlain on ArcticDEM.

Fig. 11. Elevational windows showing the inferred post-LGM thinning of the ice stream surface and geomorphology produced at each window in 79N. Arrows in A highlight inferred palaeo-ice flow directions, and extent is show in Fig. 2. Elevations refer to height of the ice stream margin above sea level. A 1° surface slope has been applied to the ice surface in these figures, similar to the currently observed ice surface slope of NEGIS. Geomorphological symbols are shown in Fig. 4.

Fig. 12. Elevational windows showing the inferred post-LGM thinning of the ice stream surface and geomorphology produced at each window on southern Lambert Land. Arrows in A highlight inferred palaeo-ice flow directions, and extent is show in Fig. 2. Elevations refer to height of the ice stream margin above sea level. A 1° surface slope has been applied to the ice surface in these figures, similar to the currently observed ice surface slope of NEGIS. Geomorphological symbols are shown in Fig. 4.

Fig. 13. Conceptual diagrams of (A) Ice stream to ice shelf deglacial transition marked along fjord walls by lateral moraines, streamlined grounding lines and delta staircases; and (B) The LIA/contemporary ice shelf margin characterised by ice shelf compressional ridges, push and controlled moraines; kames terraces; kame and kettle dead-ice terrain; ice marginal glaciofluvial corridors, and supraglacial drainage.

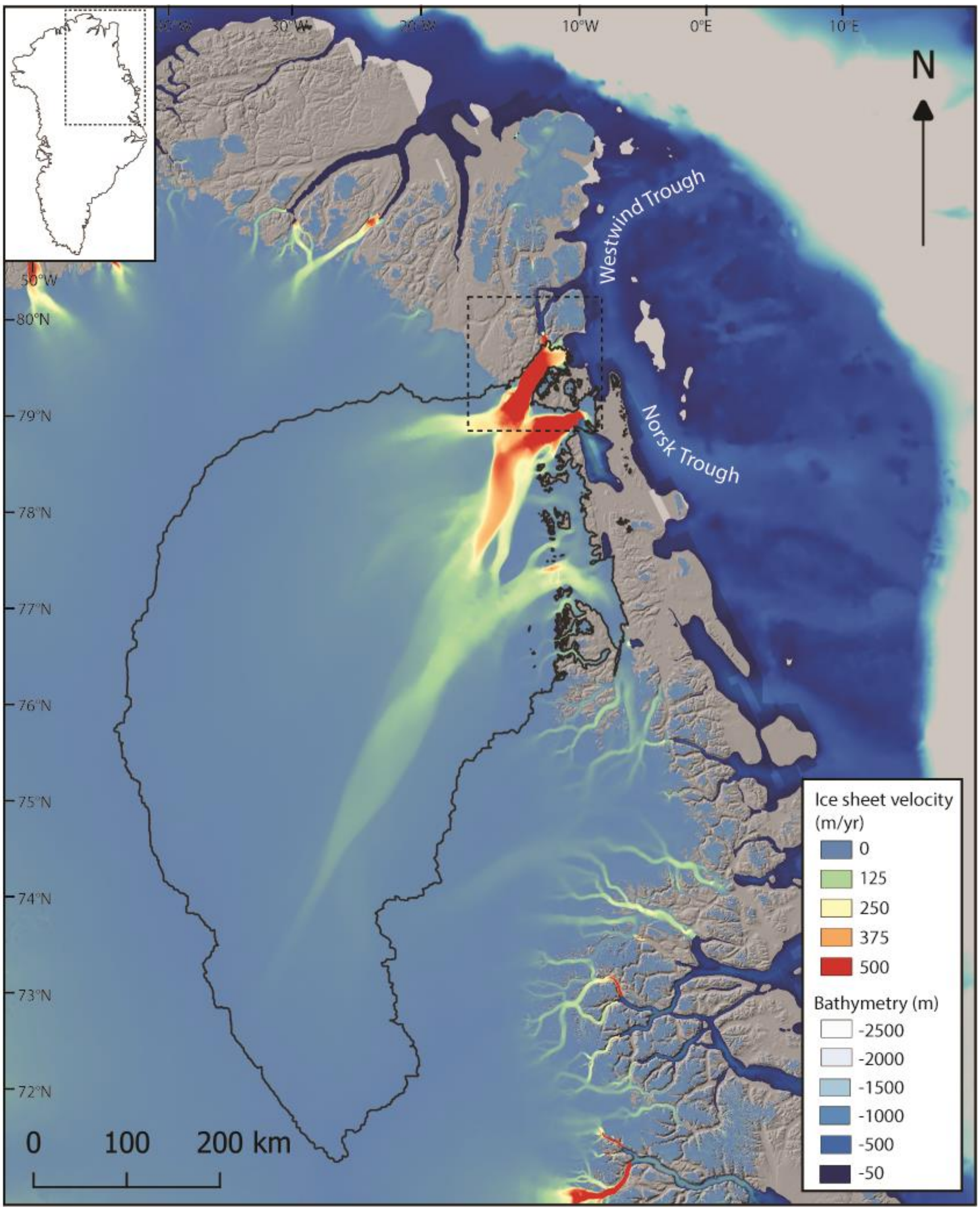
30°W
10°W
0°E
10°E
N
Westwind Trough
Norsk Trough
50°W
80°N
79°N
78°N
77°N
76°N
75°N
74°N
73°N
72°N
0
100
200 km
Ice sheet velocity (m/yr)
0
125
250
375
500
Bathymetry (m)
-2500
-2000
-1500
-1000
-500
-50

Figure 1.

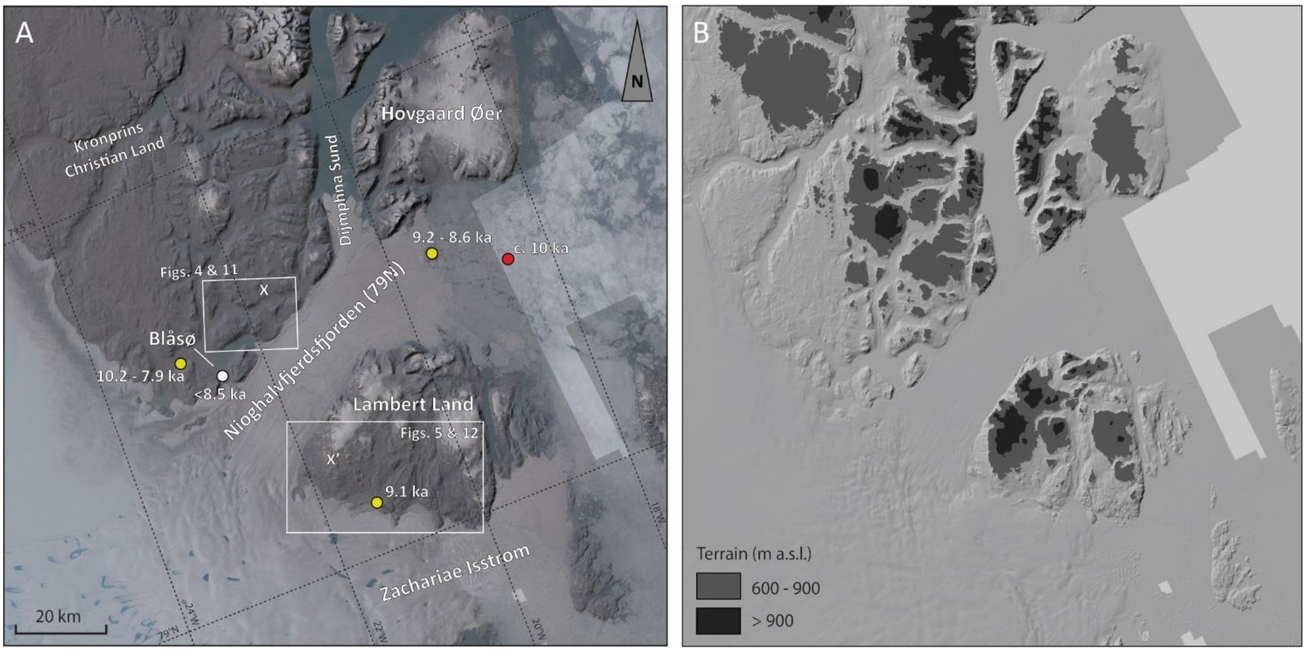
A
N
Hovgaard Øer
Kronprins Christian Land
Dijmphna Sund
9.2 - 8.6 ka
c. 10 ka
Figs. 4 & 11
X
Blåsø
10.2 - 7.9 ka
<8.5 ka
Nioghalvfjerdsfjorden (79N)
Lambert Land
Figs. 5 & 12
X'
9.1 ka
Zachariae Isstrom
20 km
B
Terrain (m a.s.l.)
600 - 900
> 900

Figure 2.

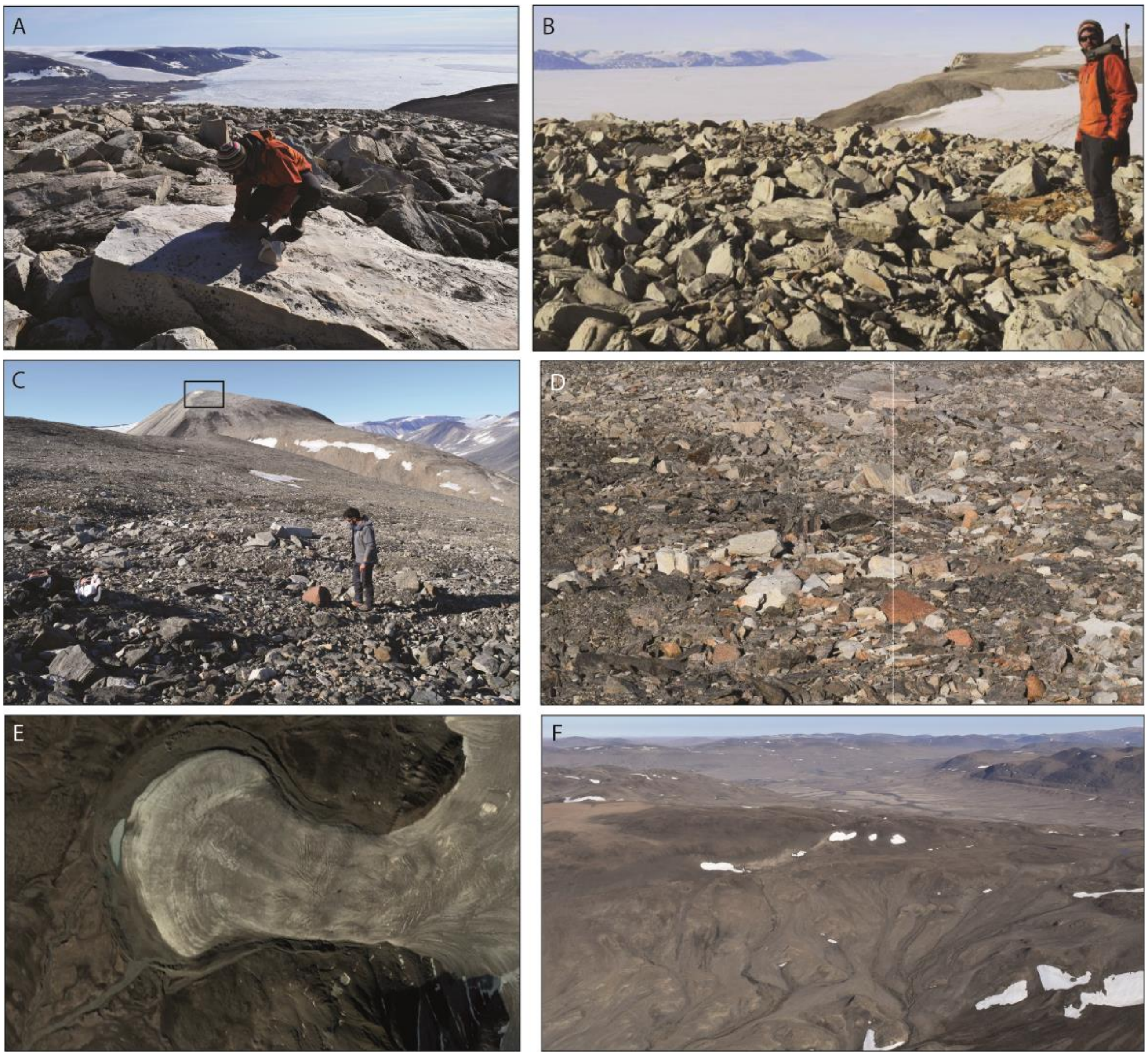

839

840 Figure 3.

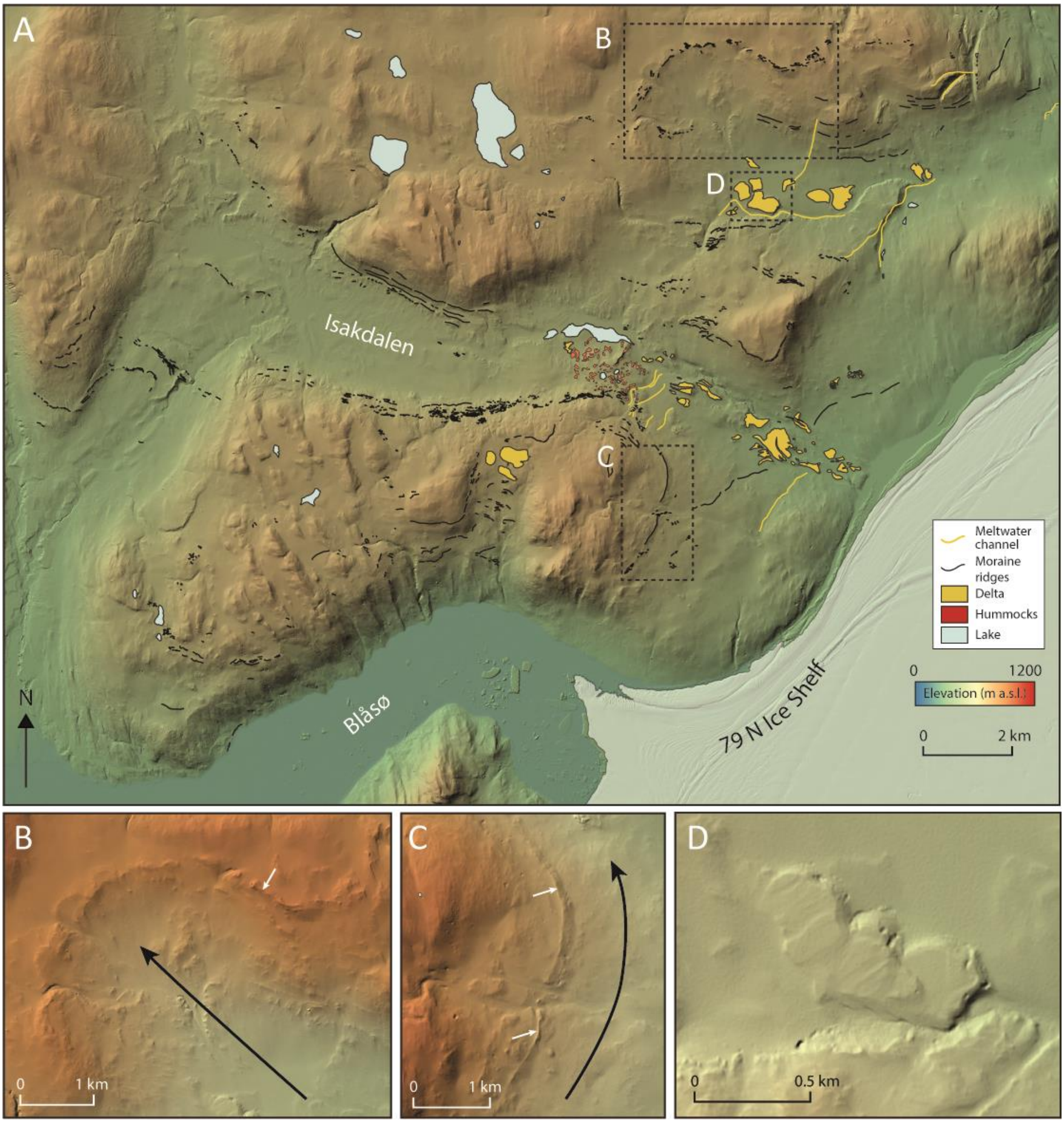

A
B
C
D
Isakdalen
Blåsø
79 N Ice Shelf
N
Meltwater channel
Moraine ridges
Delta
Hummocks
Lake
0
1200
Elevation (m a.s.l.)
0
2 km
B
0
1 km
C
0
1 km
D
0
0.5 km

Figure 4.

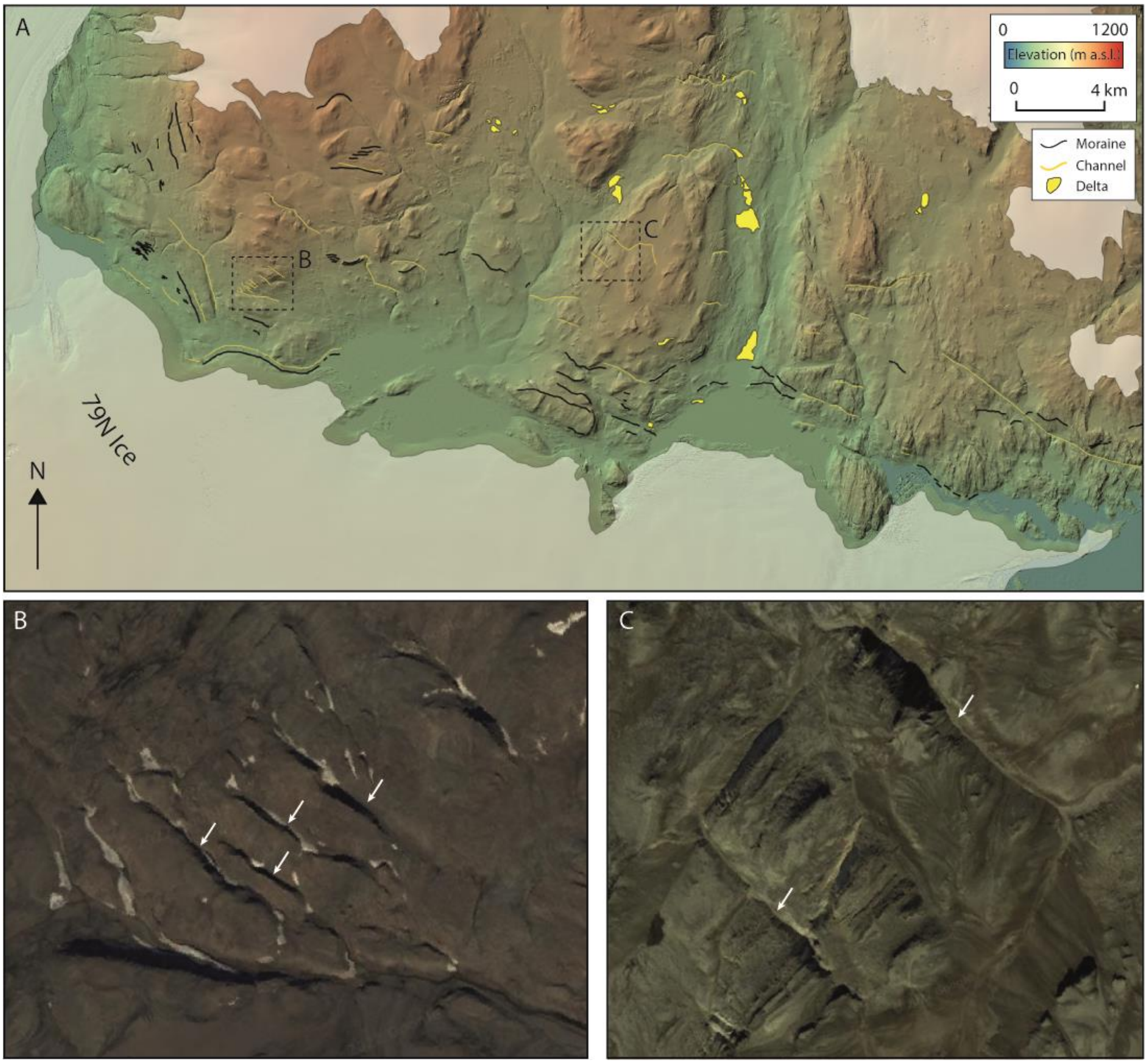
A
0
1200
Elevation (m a.s.l.)
0
4 km
Moraine
Channel
Delta
B
C
79N Ice
N
B
C

Figure 5.

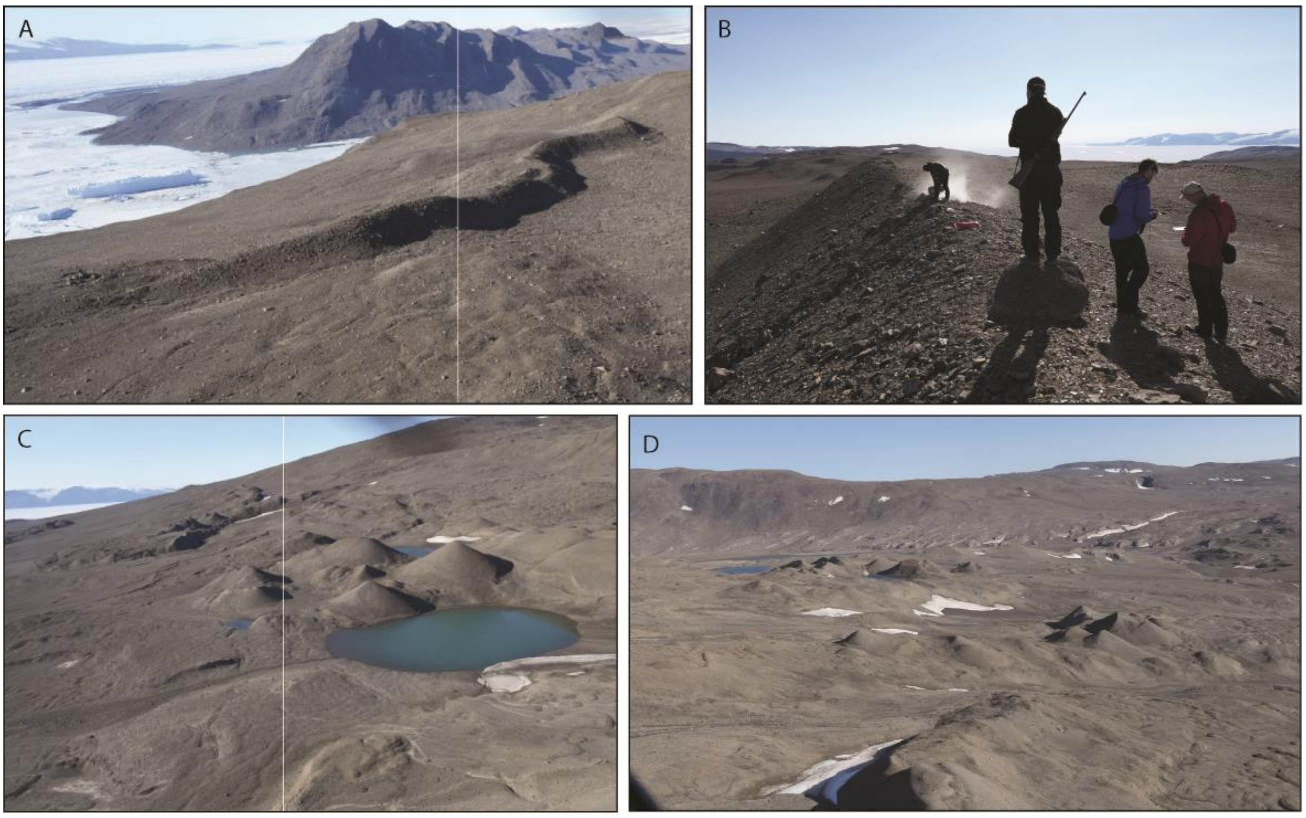

Figure 6.

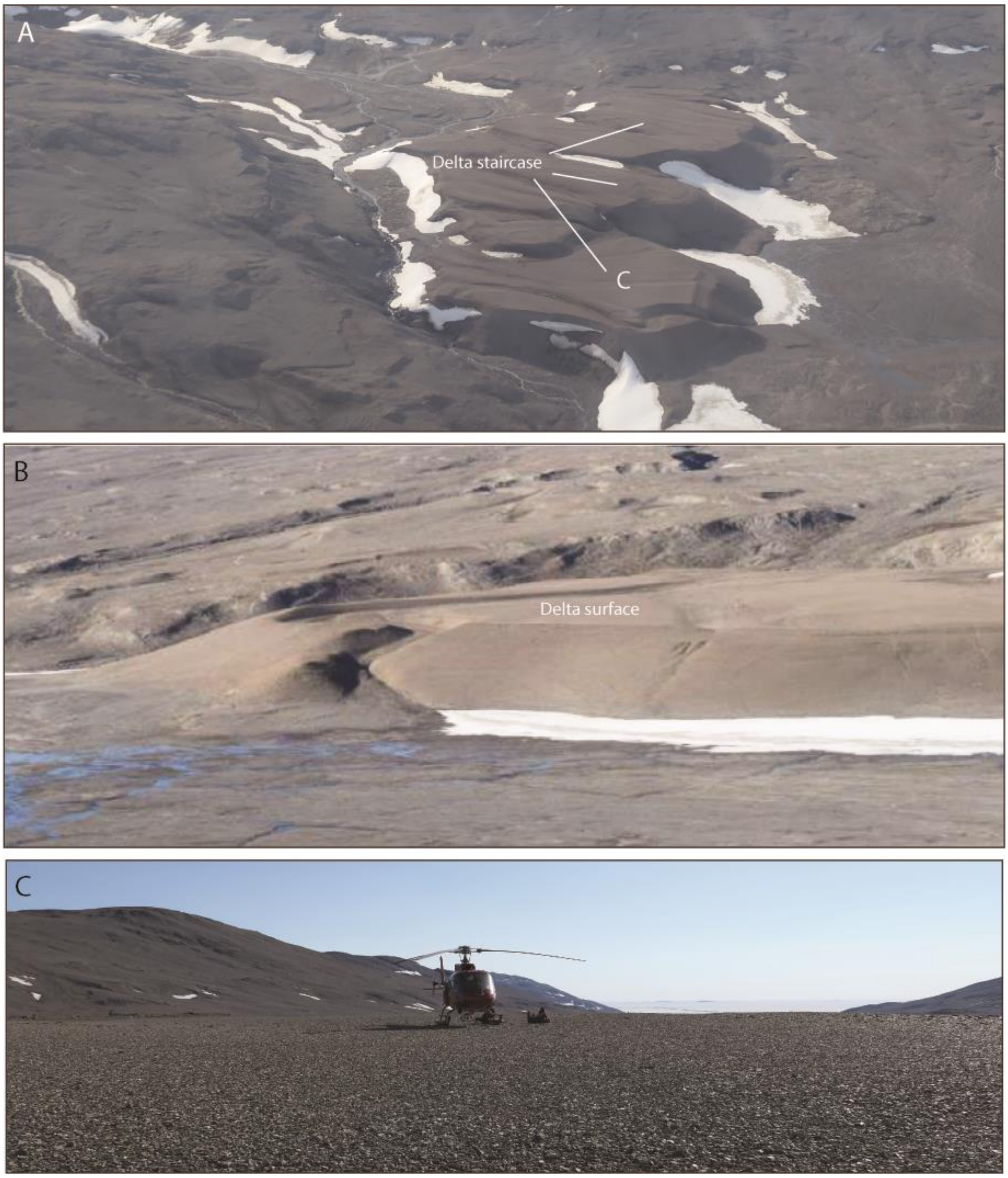

Figure 7.

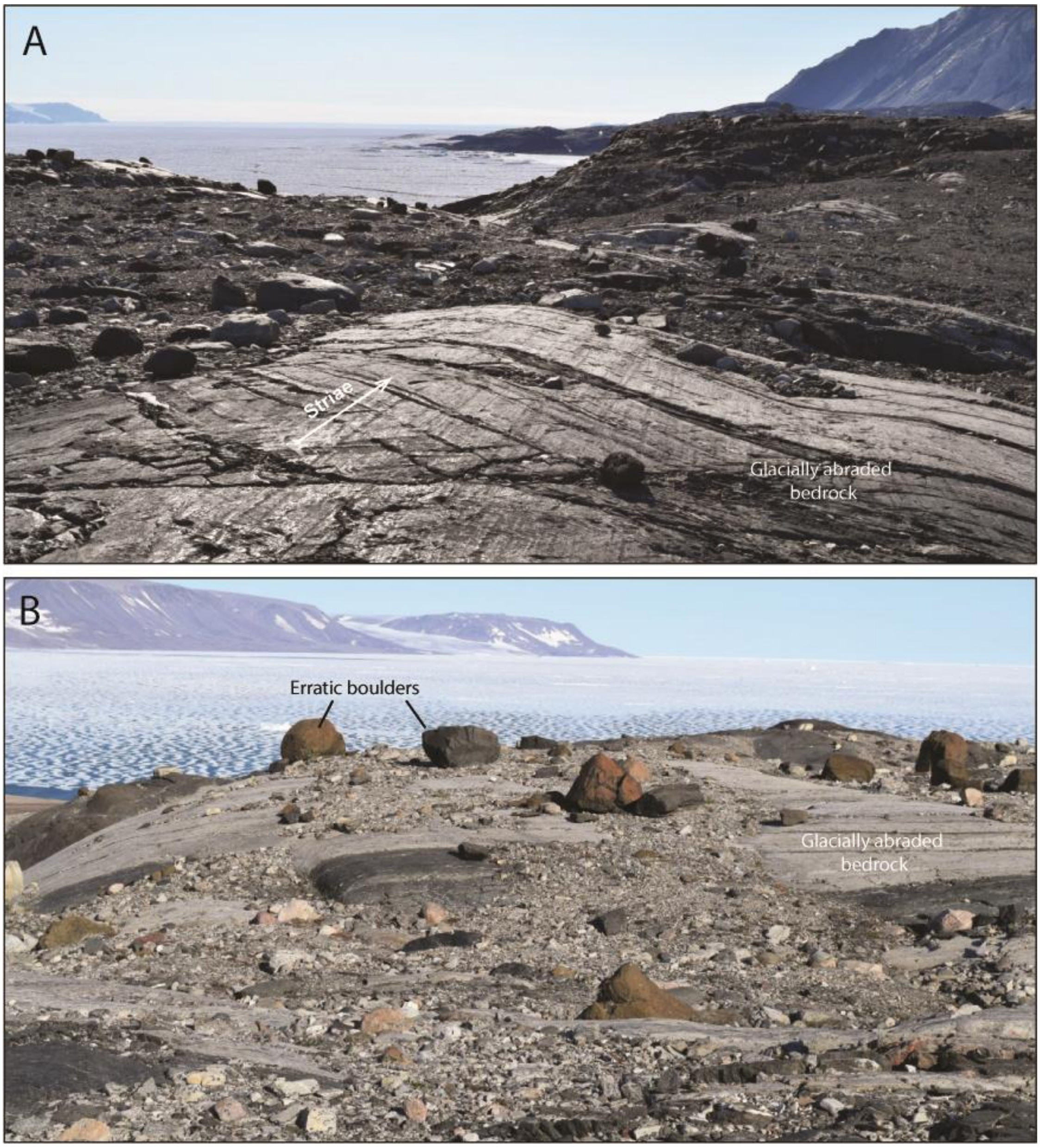
A
Striae
Glacially abraded
bedrock
B
Erratic boulders
Glacially abraded
bedrock

Figure 8.

Figure 9.

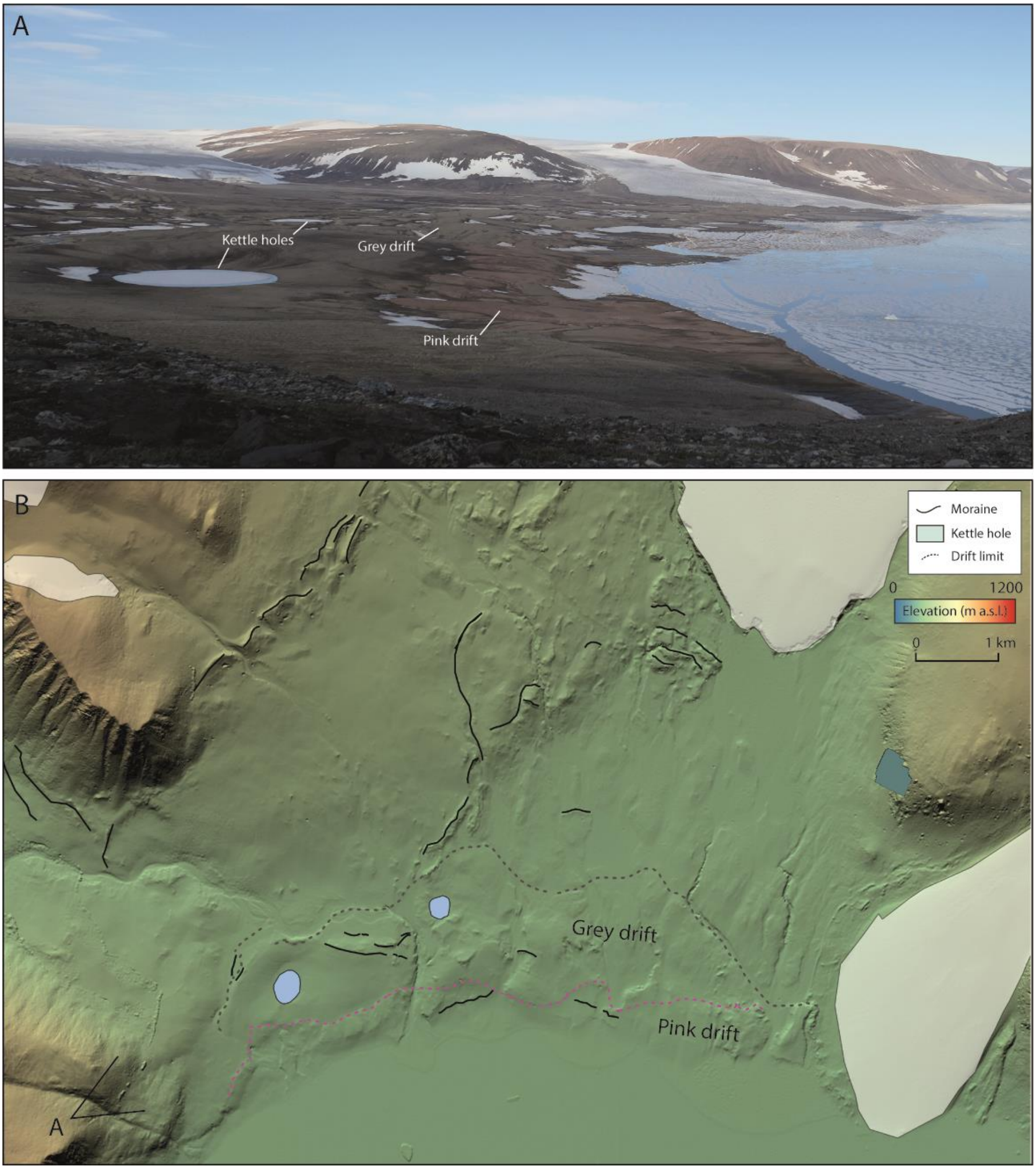

854

855 Figure 10.

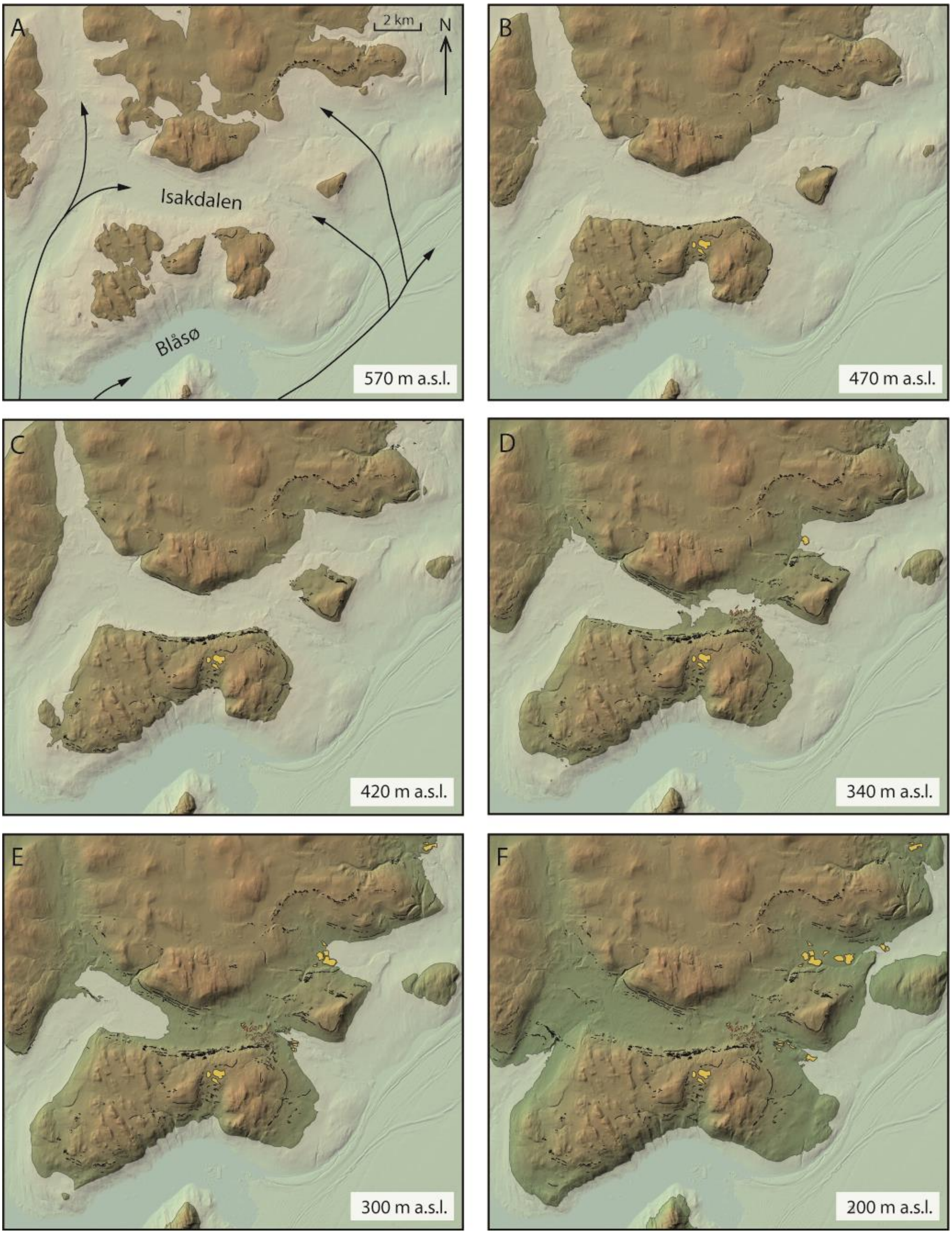
A
2 km
N
Isakdalen
Blåsø
570 m a.s.l.
B
470 m a.s.l.
C
420 m a.s.l.
D
340 m a.s.l.
E
300 m a.s.l.
F
200 m a.s.l.

Figure 11.

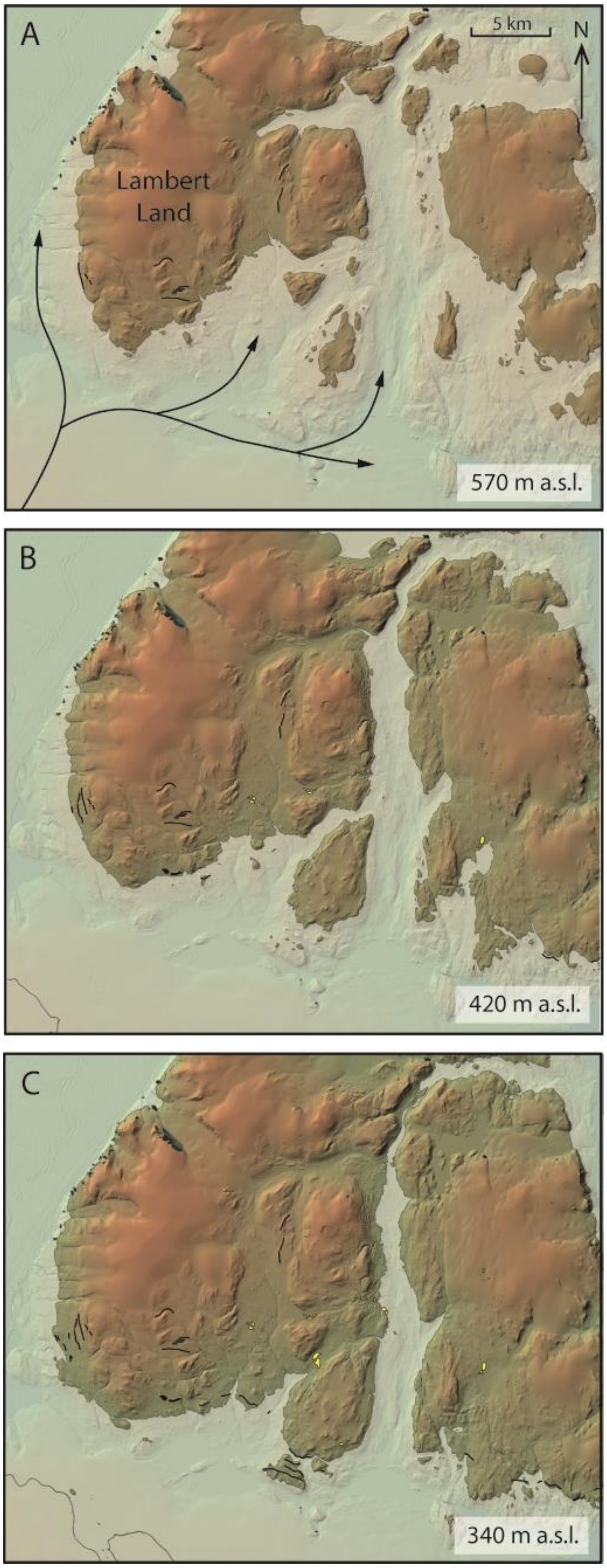

Figure 12.

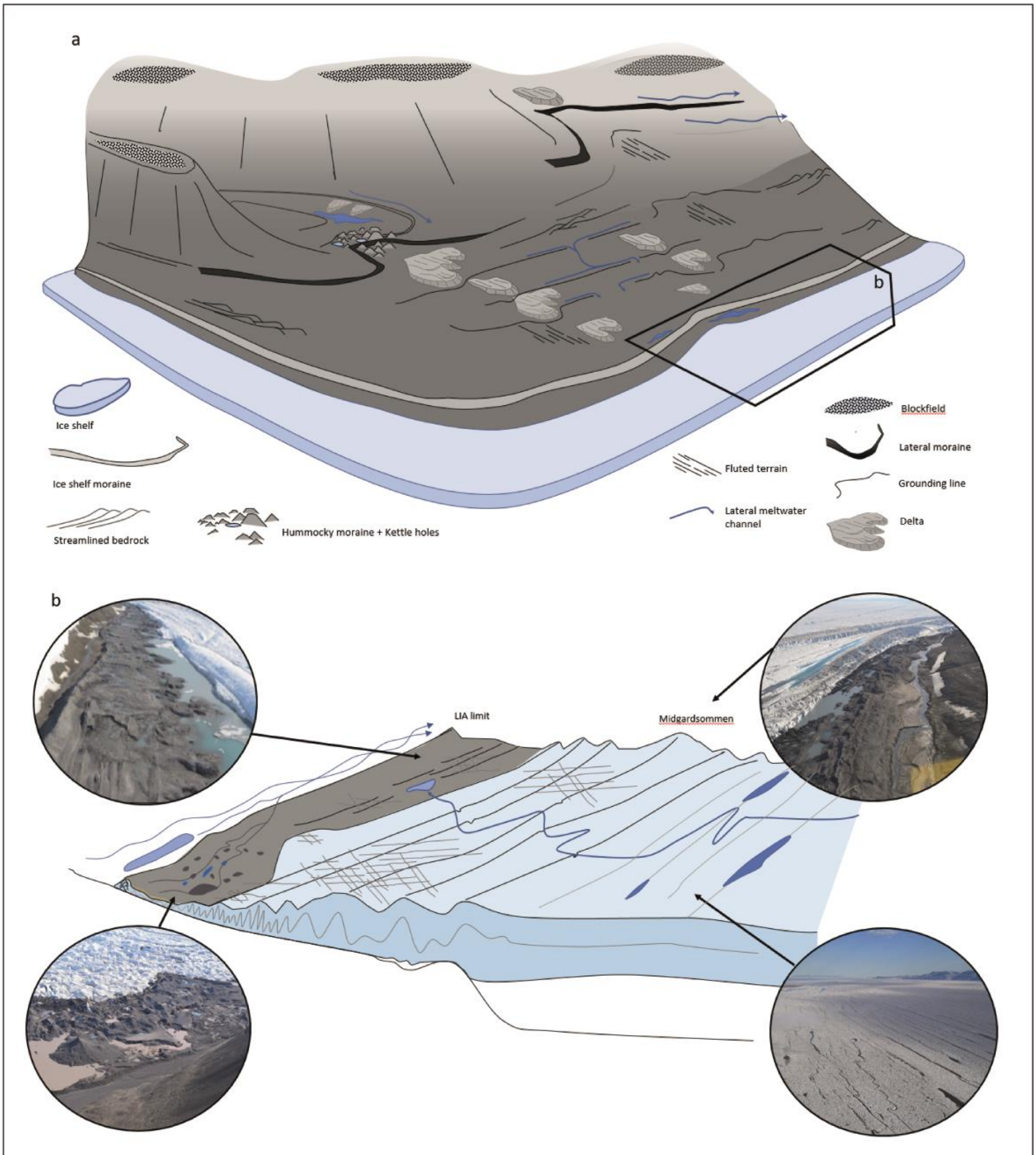

a
b
Ice shelf
Ice shelf moraine
Streamlined bedrock
Hummocky moraine + Kettle holes
Fluted terrain
Lateral meltwater channel
Blockfield
Lateral moraine
Grounding line
Delta
LIA limit
Midgardsommen

Figure 13.

REFERENCES

ANDREASSEN, K., WINSBORROW, M. C., BJARNADÓTTIR, L. R. & RÜTHER, D. C. 2014. Ice stream retreat dynamics inferred from an assemblage of landforms in the northern Barents Sea. *Quaternary Science Reviews,* 92, 246-257.

ANTONIADES, D., FRANCUS, P., PIENITZ, R., ST-ONGE, G. & VINCENT, W. F. 2011. Holocene dynamics of the Arctic's largest ice shelf. *Proceedings of the National Academy of Sciences,* 108, 18899-18904.

ARNDT, J. E., JOKAT, W. & DORSCHEL, B. 2017. The last glaciation and deglaciation of the Northeast Greenland continental shelf revealed by hydro-acoustic data. *Quaternary Science Reviews,* 160, 45-56.

ARNDT, J. E., JOKAT, W., DORSCHEL, B., MYKLEBUST, R., DOWDESWELL, J. A. & EVANS, J. 2015. A new bathymetry of the Northeast Greenland continental shelf: Constraints on glacial and other processes. *Geochemistry, Geophysics, Geosystems,* 16, 3733-3753.

BALLANTYNE, C. K. 2018. *Periglacial geomorphology*, John Wiley & Sons.

BATCHELOR, C. & DOWDESWELL, J. 2015. Ice-sheet grounding-zone wedges (GZWs) on high-latitude continental margins. *Marine Geology,* 363, 65-92.

BATCHELOR, C. & DOWDESWELL, J. 2016. Lateral shear-moraines and lateral marginal-moraines of palaeo-ice streams. *Quaternary Science Reviews,* 151, 1-26.

BAY, C. 1997. Floristical and ecological characterization of the polar desert zone of Greenland. *Journal of Vegetation Science,* 8, 685-696.

BEEL, C., LIFTON, N., BRINER, J. & GOEHRING, B. 2016. Quaternary evolution and ice sheet history of contrasting landscapes in Uummannaq and Sukkertoppen, western Greenland. *Quaternary Science Reviews,* 149, 248-258.

BENN, D. & EVANS, D. J. 2014. *Glaciers and glaciation*, Routledge.

BENN, D. I. 1992. The genesis and significance of 'hummocky moraine': evidence from the Isle of Skye, Scotland. *Quaternary Science Reviews,* 11, 781-799.

BENNIKE, O. & WEIDICK, A. 2001. Late Quaternary history around Nioghalvfjerdsfjorden and Jøkelbugten, North-East Greenland. *Boreas,* 30, 205-227.

BENTLEY, M., HODGSON, D., SUGDEN, D., ROBERTS, S., SMITH, J., LENG, M. & BRYANT, C. 2005. Early Holocene retreat of the George VI ice shelf, Antarctic Peninsula. *Geology,* 33, 173-176.

BENTLEY, M. J., SMITH, J. A., JAMIESON, S. S., LINDEMAN, M., REA, B. R., HUMBERT, A., LANE, T. P., DARVILL, C. M., LLOYD, J. M. & STRANEO, F. 2022. Direct measurement of warm Atlantic Intermediate Water close to the grounding line of Nioghalvfjerdsfjorden (79N) Glacier, North-east Greenland. *The Cryosphere Discussions*, 1-25.

BRINER, J. P., LIFTON, N. A., MILLER, G. H., REFSNIDER, K., ANDERSON, R. & FINKEL, R. 2014. Using in situ cosmogenic 10Be, 14C, and 26Al to decipher the history of polythermal ice sheets on Baffin Island, Arctic Canada. *Quaternary Geochronology,* 19, 4-13.

BRINER, J. P., MCKAY, N. P., AXFORD, Y., BENNIKE, O., BRADLEY, R. S., DE VERNAL, A., FISHER, D., FRANCUS, P., FRÉCHETTE, B. & GAJEWSKI, K. 2016. Holocene climate change in Arctic Canada and Greenland. *Quaternary Science Reviews,* 147, 340-364.

CHANDLER, B. M., LOVELL, H., BOSTON, C. M., LUKAS, S., BARR, I. D., BENEDIKTSSON, Í. Ö., BENN, D. I., CLARK, C. D., DARVILL, C. M. & EVANS, D. J. 2018. Glacial geomorphological mapping: A review of approaches and frameworks for best practice. *Earth-Science Reviews,* 185, 806-846.

CHOI, Y., MORLIGHEM, M., RIGNOT, E., MOUGINOT, J. & WOOD, M. 2017. Modeling the response of Nioghalvfjerdsfjorden and Zachariae Isstrøm glaciers, Greenland, to ocean forcing over the next century. *Geophysical Research Letters,* 44, 11,071-11,079.

COUETTE, P.-O., LAJEUNESSE, P., GHIENNE, J.-F., DORSCHEL, B., GEBHARDT, C., HEBBELN, D. & BROUARD, E. 2022. Evidence for an extensive ice shelf in northern Baffin Bay during the Last Glacial Maximum. *Communications Earth & Environment,* 3**,** 1-12.

DAHL, R. 1966. Block fields, weathering pits and tor-like forms in the Narvik Mountains, Nordland, Norway. *Geografiska Annaler: Series A, Physical Geography,* 48**,** 55-85.

DAVIES, B. J., HAMBREY, M. J., GLASSER, N. F., HOLT, T., RODÉS, A., SMELLIE, J. L., CARRIVICK, J. L. & BLOCKLEY, S. P. 2017. Ice-dammed lateral lake and epishelf lake insights into Holocene dynamics of Marguerite trough ice stream and George VI ice shelf, Alexander island, Antarctic peninsula. *Quaternary Science Reviews,* 177**,** 189-219.

DAVIES, J., MATHIASEN, A. M., KRISTIANSEN, K., HANSEN, K. E., WACKER, L., ALSTRUP, A. K. O., MUNK, O. L., PEARCE, C. & SEIDENKRANTZ, M.-S. 2022. Linkages between ocean circulation and the Northeast Greenland Ice Stream in the Early Holocene. *Quaternary Science Reviews,* 286**,** 107530.

DOWDESWELL, J., BATCHELOR, C., MONTELLI, A., OTTESEN, D., CHRISTIE, F., DOWDESWELL, E. & EVANS, J. 2020. Delicate seafloor landforms reveal past Antarctic grounding-line retreat of kilometers per year. *Science,* 368**,** 1020-1024.

DOWDESWELL, J. & FUGELLI, E. 2012. The seismic architecture and geometry of grounding-zone wedges formed at the marine margins of past ice sheets. *Bulletin,* 124**,** 1750-1761.

DOWDESWELL, J. A. & JEFFRIES, M. O. 2017. Arctic ice shelves: An introduction. *Arctic ice shelves and ice islands.* Springer.

ENGLAND, J., BRADLEY, R. S. & MILLER, G. 1978. Former ice shelves in the Canadian High Arctic. *Journal of Glaciology,* 20**,** 393-404.

ENGLAND, J., COULTHARD, R., FURZE, M. & DOW, C. 2022. Catastrophic ice shelf collapse along the NW Laurentide Ice Sheet highlights the vulnerability of marine-based ice margins. *Quaternary Science Reviews,* 286**,** 107524.

ENGLAND, J. H., FURZE, M. F. & DOUPE, J. P. 2009. Revision of the NW Laurentide Ice Sheet: implications for paleoclimate, the northeast extremity of Beringia, and Arctic Ocean sedimentation. *Quaternary Science Reviews,* 28**,** 1573-1596.

EVANS, D. J. 2009. Controlled moraines: origins, characteristics and palaeoglaciological implications. *Quaternary Science Reviews,* 28**,** 183-208.

EVANS, D. J., HUGHES, A. L., HANSOM, J. D. & ROBERTS, D. H. 2017. Scottish landform examples 43: Glacifluvial landforms of Strathallan, Perthshire. *Scottish Geographical Journal,* 133**,** 42-53.

EVANS, D. J., REA, B. R., HANSOM, J. D. & WHALLEY, W. B. 2002. Geomorphology and style of plateau icefield deglaciation in fjord terrains: the example of Troms-Finnmark, north Norway. *Journal of Quaternary Science: Published for the Quaternary Research Association,* 17**,** 221-239.

EVANS, D. J., STORRAR, R. D. & REA, B. R. 2016. Crevasse-squeeze ridge corridors: diagnostic features of late-stage palaeo-ice stream activity. *Geomorphology,* 258**,** 40-50.

EVANS, J., Ó COFAIGH, C., DOWDESWELL, J. A. & WADHAMS, P. 2009. Marine geophysical evidence for former expansion and flow of the Greenland Ice Sheet across the north-east Greenland continental shelf. *Journal of Quaternary Science: Published for the Quaternary Research Association,* 24**,** 279-293.

FAHNESTOCK, M., BINDSCHADLER, R., KWOK, R. & JEZEK, K. 1993. Greenland ice sheet surface properties and ice dynamics from ERS-1 SAR imagery. *Science,* 262**,** 1530-1534.

FRANKE, S., JANSEN, D., BINDER, T., DÖRR, N., HELM, V., PADEN, J., STEINHAGE, D. & EISEN, O. 2020. Bed topography and subglacial landforms in the onset region of the Northeast Greenland Ice Stream. *Annals of Glaciology,* 61**,** 143-153.

FREIRE, F., GYLLENCREUTZ, R., GREENWOOD, S. L., MAYER, L., EGILSSON, A., THORSTEINSSON, T. & JAKOBSSON, M. 2015. High resolution mapping of offshore and onshore glaciogenic features in metamorphic bedrock terrain, Melville Bay, northwestern Greenland. *Geomorphology,* 250, 29-40.

FURZE, M. F., PIEŃKOWSKI, A. J., MCNEELY, M. A., BENNETT, R. & CAGE, A. G. 2018. Deglaciation and ice shelf development at the northeast margin of the Laurentide Ice Sheet during the Younger Dryas chronozone. *Boreas,* 47, 271-296.

GARDNER, A., FAHNESTOCK, M. & SCAMBOS, T. 2019. ITS_LIVE Regional Glacier and Ice Sheet Surface Velocities, National Snow and Ice Data Center.

GARDNER, A. S., MOHOLDT, G., SCAMBOS, T., FAHNSTOCK, M., LIGTENBERG, S., VAN DEN BROEKE, M. & NILSSON, J. 2018. Increased West Antarctic and unchanged East Antarctic ice discharge over the last 7 years. *The Cryosphere,* 12, 521-547.

GIBSON, J. A. & ANDERSEN, D. T. 2002. Physical structure of epishelf lakes of the southern Bunger Hills, East Antarctica. *Antarctic Science,* 14, 253-261.

GLASSER, N., GOODSELL, B., COPLAND, L. & LAWSON, W. 2006. Debris characteristics and ice-shelf dynamics in the ablation region of the McMurdo Ice Shelf, Antarctica. *Journal of Glaciology,* 52, 223-234.

GOLDBERG, D., HOLLAND, D. & SCHOOF, C. 2009. Grounding line movement and ice shelf buttressing in marine ice sheets. *Journal of Geophysical Research: Earth Surface,* 114.

GRAHAM, A. G., LARTER, R. D., GOHL, K., HILLENBRAND, C.-D., SMITH, J. A. & KUHN, G. 2009. Bedform signature of a West Antarctic palaeo-ice stream reveals a multi-temporal record of flow and substrate control. *Quaternary Science Reviews,* 28, 2774-2793.

GUDMUNDSSON, G. 2013. Ice-shelf buttressing and the stability of marine ice sheets. *The Cryosphere,* 7, 647-655.

HAMBREY, M. J., DAVIES, B. J., GLASSER, N. F., HOLT, T. O., SMELLIE, J. L. & CARRIVICK, J. L. 2015. Structure and sedimentology of George VI Ice Shelf, Antarctic Peninsula: implications for ice-sheet dynamics and landform development. *Journal of the Geological Society,* 172, 599-613.

HODGSON, D. A. & VINCENT, J.-S. 1984. A 10,000 yr BP extensive ice shelf over Viscount Melville Sound, Arctic Canada. *Quaternary Research,* 22, 18-30.

HOGG, A. E., SHEPHERD, A., GOURMELEN, N. & ENGDAHL, M. 2016. Grounding line migration from 1992 to 2011 on Petermann glacier, North-West Greenland. *Journal of Glaciology,* 62, 1104-1114.

JEZEK, K., WU, X., GOGINENI, P., RODRÍGUEZ, E., FREEMAN, A., RODRIGUEZ-MORALES, F. & CLARK, C. D. 2011. Radar images of the bed of the Greenland Ice Sheet. *Geophysical Research Letters,* 38.

JOHNSON, J. S., BENTLEY, M. J., SMITH, J. A., FINKEL, R., ROOD, D., GOHL, K., BALCO, G., LARTER, R. D. & SCHAEFER, J. 2014. Rapid thinning of Pine Island Glacier in the early Holocene. *Science,* 343, 999-1001.

JOUGHIN, I., SMITH, B. E., HOWAT, I. M., SCAMBOS, T. & MOON, T. 2010. Greenland flow variability from ice-sheet-wide velocity mapping. *Journal of Glaciology,* 56, 415-430.

KAUFMAN, D. S., AGER, T. A., ANDERSON, N. J., ANDERSON, P. M., ANDREWS, J. T., BARTLEIN, P. J., BRUBAKER, L. B., COATS, L. L., CWYNAR, L. C. & DUVALL, M. L. 2004. Holocene thermal maximum in the western Arctic (0–180 W). *Quaternary Science Reviews,* 23, 529-560.

KESSLER, M. A., ANDERSON, R. S. & BRINER, J. P. 2008. Fjord insertion into continental margins driven by topographic steering of ice. *Nature Geoscience,* 1, 365-369.

KHAN, S. A., KJÆR, K. H., BEVIS, M., BAMBER, J. L., WAHR, J., KJELDSEN, K. K., BJØRK, A. A., KORSGAARD, N. J., STEARNS, L. A. & VAN DEN BROEKE, M. R. 2014. Sustained mass loss of the northeast Greenland ice sheet triggered by regional warming. *Nature Climate Change,* 4**,** 292-299.

KLEMAN, J., HÄTTESTRAND, C., BORGSTRÖM, I. & STROEVEN, A. 1997. Fennoscandian palaeoglaciology reconstructed using a glacial geological inversion model. *Journal of glaciology,* 43**,** 283-299.

LANE, T. P., ROBERTS, D. H., Ó COFAIGH, C., REA, B. R. & VIELI, A. 2016. Glacial landscape evolution in the Uummannaq region, West Greenland. *Boreas,* 45**,** 220-234.

LANE, T. P., ROBERTS, D. H., Ó COFAIGH, C., VIELI, A. & MORETON, S. G. 2015a. The glacial history of the southern Svartenhuk Halvø, West Greenland. *arktos,* 1**,** 1-28.

LANE, T. P., ROBERTS, D. H., REA, B. R., COFAIGH, C. Ó. & VIELI, A. 2015b. Controls on bedrock bedform development beneath the Uummannaq Ice Stream onset zone, West Greenland. *Geomorphology,* 231**,** 301-313.

LANE, T. P., ROBERTS, D. H., REA, B. R., COFAIGH, C. Ó., VIELI, A. & RODÉS, A. 2014. Controls upon the Last Glacial maximum deglaciation of the northern Uummannaq ice stream system, West Greenland. *Quaternary Science Reviews,* 92**,** 324-344.

LARSEN, N. K., KJÆR, K. H., FUNDER, S., MÖLLER, P., VAN DER MEER, J. J., SCHOMACKER, A., LINGE, H. & DARBY, D. A. 2010. Late Quaternary glaciation history of northernmost Greenland–Evidence of shelf-based ice. *Quaternary Science Reviews,* 29**,** 3399-3414.

LARSEN, N. K., LEVY, L. B., CARLSON, A. E., BUIZERT, C., OLSEN, J., STRUNK, A., BJØRK, A. A. & SKOV, D. S. 2018. Instability of the Northeast Greenland Ice Stream over the last 45,000 years. *Nature communications,* 9**,** 1-8.

LEA, J. M., MAIR, D. W., NICK, F. M., REA, B. R., WEIDICK, A., KJAER, K. H., MORLIGHEM, M., VAN AS, D. & SCHOFIELD, J. E. 2014. Terminus-driven retreat of a major southwest Greenland tidewater glacier during the early 19th century: insights from glacier reconstructions and numerical modelling. *Journal of Glaciology,* 60**,** 333-344.

MACKINTOSH, A. N., VERLEYEN, E., O'BRIEN, P. E., WHITE, D. A., JONES, R. S., MCKAY, R., DUNBAR, R., GORE, D. B., FINK, D. & POST, A. L. 2014. Retreat history of the East Antarctic Ice Sheet since the last glacial maximum. *Quaternary Science Reviews,* 100**,** 10-30.

MAYER, C., SCHAFFER, J., HATTERMANN, T., FLORICIOIU, D., KRIEGER, L., DODD, P. A., KANZOW, T., LICCIULLI, C. & SCHANNWELL, C. 2018. Large ice loss variability at Nioghalvfjerdsfjorden glacier, northeast-Greenland. *Nature communications,* 9**,** 1-11.

MÖLLER, P., LARSEN, N. K., KJÆR, K. H., FUNDER, S., SCHOMACKER, A., LINGE, H. & FABEL, D. 2010. Early to middle Holocene valley glaciations on northernmost Greenland. *Quaternary Science Reviews,* 29**,** 3379-3398.

MOON, T., FISHER, M., HARDEN, L. & STAFFORD, T. 2021. QGreenland (v1.0.1) [software]. . Available from https://qgreenland.org. .

MORLIGHEM, M., WILLIAMS, C. N., RIGNOT, E., AN, L., ARNDT, J. E., BAMBER, J. L., CATANIA, G., CHAUCHÉ, N., DOWDESWELL, J. A. & DORSCHEL, B. 2017. BedMachine v3: Complete bed topography and ocean bathymetry mapping of Greenland from multibeam echo sounding combined with mass conservation. *Geophysical research letters,* 44**,** 11,051-11,061.

MOUGINOT, J., RIGNOT, E., SCHEUCHL, B., FENTY, I., KHAZENDAR, A., MORLIGHEM, M., BUZZI, A. & PADEN, J. 2015. Fast retreat of Zachariæ Isstrøm, northeast Greenland. *Science,* 350**,** 1357-1361.

NEWTON, A., KNUTZ, P., HUUSE, M., GANNON, P., BROCKLEHURST, S., CLAUSEN, O. & GONG, Y. 2017. Ice stream reorganization and glacial retreat on the northwest Greenland shelf. *Geophysical Research Letters,* 44**,** 7826-7835.

NIELSEN, L. T., AÐALGEIRSDÓTTIR, G., GKINIS, V., NUTERMAN, R. & HVIDBERG, C. S. 2018. The effect of a Holocene climatic optimum on the evolution of the Greenland ice sheet during the last 10 kyr. *Journal of Glaciology,* 64**,** 477-488.

Ó COFAIGH, C., DOWDESWELL, J., JENNINGS, A., HOGAN, K., KILFEATHER, A., HIEMSTRA, J., NOORMETS, R., EVANS, J., MCCARTHY, D. & ANDREWS, J. 2013. An extensive and dynamic ice sheet on the West Greenland shelf during the last glacial cycle. *Geology,* 41**,** 219-222.

Ó COFAIGH, C., DOWDESWELL, J. A., EVANS, J. & LARTER, R. D. 2008. Geological constraints on Antarctic palaeo-ice-stream retreat. *Earth Surface Processes and Landforms: The Journal of the British Geomorphological Research Group,* 33**,** 513-525.

Ó COFAIGH, C., EVANS, J., DOWDESWELL, J. A. & LARTER, R. D. 2007. Till characteristics, genesis and transport beneath Antarctic paleo-ice streams. *Journal of Geophysical Research: Earth Surface,* 112.

Ó COFAIGH, C., PUDSEY, C. J., DOWDESWELL, J. A. & MORRIS, P. 2002. Evolution of subglacial bedforms along a paleo-ice stream, Antarctic Peninsula continental shelf. *Geophysical Research Letters,* 29**,** 41-1-41-4.

PEARCE, D. M., MAIR, D. W., REA, B. R., LEA, J. M., SCHOFIELD, J. E., KAMENOS, N. & SCHOENROCK, K. 2018. The glacial geomorphology of upper Godthåbsfjord (Nuup Kangerlua) in southwest Greenland. *Journal of Maps,* 14**,** 45-55.

PEDERSEN, M., WENG, W. L., KEULEN, N. & KOKFELT, T. F. 2013. A new seamless digital 1: 500 000 scale geological map of Greenland. *GEUS Bulletin,* 28**,** 65-68.

REA, B. R., WHALLEY, W. B., EVENS, D., GORDON, J. E. & MCDOUGALL, D. A. 1998. Plateau icefields: geomorphology and dynamics. *Journal of Quaternary Science,* 13**,** 35-54.

REA, B. R., WHALLEY, W. B., RAINEY, M. M. & GORDON, J. E. 1996. Blockfields, old or new? Evidence and implications from some plateaus in northern Norway. *Geomorphology,* 15**,** 109-121.

REESE, R., GUDMUNDSSON, G. H., LEVERMANN, A. & WINKELMANN, R. 2018. The far reach of ice-shelf thinning in Antarctica. *Nature Climate Change,* 8**,** 53-57.

RIGNOT, E., JACOBS, S., MOUGINOT, J. & SCHEUCHL, B. 2013. Ice-shelf melting around Antarctica. *Science,* 341**,** 266-270.

ROBERSON, S., HUBBARD, B., COULSON, H. R. & BOOMER, I. 2011. Physical properties and formation of flutes at a polythermal valley glacier: Midre Lovénbreen, Svalbard. *Geografiska Annaler: Series A, Physical Geography,* 93**,** 71-88.

ROBERTS, D. H. & LONG, A. 2005. Streamlined bedrock terrain and fast ice flow, Jakobshavns Isbrae, West Greenland: implications for ice stream and ice sheet dynamics. *Boreas,* 34**,** 25-42.

ROBERTS, D. H., LONG, A. J., DAVIES, B. J., SIMPSON, M. J. & SCHNABEL, C. 2010. Ice stream influence on west Greenland ice sheet dynamics during the last glacial maximum. *Journal of Quaternary Science,* 25**,** 850-864.

ROBERTS, D. H., REA, B. R., LANE, T. P., SCHNABEL, C. & RODÉS, A. 2013. New constraints on Greenland ice sheet dynamics during the last glacial cycle: evidence from the Uummannaq ice stream system. *Journal of Geophysical Research: Earth Surface,* 118**,** 519-541.

ROBERTS, S., HODGSON, D., BENTLEY, M., SMITH, J., MILLAR, I., OLIVE, V. & SUGDEN, D. E. 2008. The Holocene history of George VI Ice Shelf, Antarctic Peninsula from clast-provenance analysis of epishelf lake sediments. *Palaeogeography, Palaeoclimatology, Palaeoecology,* 259**,** 258-283.

SCAMBOS, T. A., BOHLANDER, J., SHUMAN, C. A. & SKVARCA, P. 2004. Glacier acceleration and thinning after ice shelf collapse in the Larsen B embayment, Antarctica. *Geophysical Research Letters,* 31.

SCHAFFER, J., KANZOW, T., VON APPEN, W.-J., VON ALBEDYLL, L., ARNDT, J. E. & ROBERTS, D. H. 2020. Bathymetry constrains ocean heat supply to Greenland's largest glacier tongue. *Nature Geoscience,* 13**,** 227-231.

SKOV, D. S., ANDERSEN, J., OLSEN, J., JACOBSEN, B., KNUDSEN, M., JANSEN, J., LARSEN, N. & EGHOLM, D. 2020. Constraints from cosmogenic nuclides on the glaciation and erosion history of Dove Bugt, northeast Greenland. *GSA Bulletin,* 132**,** 2282-2294.

SMITH, J. A., ANDERSEN, T., SHORTT, M., GAFFNEY, A., TRUFFER, M., STANTON, T. P., BINDSCHADLER, R., DUTRIEUX, P., JENKINS, A. & HILLENBRAND, C.-D. 2017. Sub-ice-shelf sediments record history of twentieth-century retreat of Pine Island Glacier. *Nature,* 541**,** 77-80.

SMITH, J. A., BENTLEY, M. J., HODGSON, D. A., ROBERTS, S. J., LENG, M. J., LLOYD, J. M., BARRETT, M. S., BRYANT, C. & SUGDEN, D. E. 2007. Oceanic and atmospheric forcing of early Holocene ice shelf retreat, George VI Ice Shelf, Antarctica Peninsula. *Quaternary Science Reviews,* 26**,** 500-516.

SMITH, J. A., CALLARD, L., BENTLEY, M. J., JAMIESON, S. S., SÁNCHEZ-MONTES, M. L., LANE, T. P., LLOYD, J. M., MCCLYMONT, E. L., DARVILL, C. M. & REA, B. R. 2022. Holocene history of 79° N ice shelf reconstructed from epishelf lake and uplifted glacimarine sediments. *The Cryosphere Discussions***,** 1-38.

SMITH, J. A., GRAHAM, A. G., POST, A. L., HILLENBRAND, C.-D., BART, P. J. & POWELL, R. D. 2019. The marine geological imprint of Antarctic ice shelves. *Nature Communications,* 10**,** 1-16.

SMITH, J. A., HODGSON, D. A., BENTLEY, M. J., VERLEYEN, E., LENG, M. J. & ROBERTS, S. J. 2006. Limnology of two Antarctic epishelf lakes and their potential to record periods of ice shelf loss. *Journal of Paleolimnology,* 35**,** 373-394.

STEIN, R., NAM, S.-I., GROBE, H. & HUBBERTEN, H. 1996. Late Quaternary glacial history and short-term ice-rafted debris fluctuations along the East Greenland continental margin. *Geological Society, London, Special Publications,* 111**,** 135-151.

STOKES, C. R. & CLARK, C. D. 2003. The Dubawnt Lake palaeo-ice stream: evidence for dynamic ice sheet behaviour on the Canadian Shield and insights regarding the controls on ice-stream location and vigour. *Boreas,* 32**,** 263-279.

STRUNK, A., KNUDSEN, M. F., EGHOLM, D. L., JANSEN, J. D., LEVY, L. B., JACOBSEN, B. H. & LARSEN, N. K. 2017. One million years of glaciation and denudation history in west Greenland. *Nature communications,* 8**,** 1-8.

SUGDEN, D. 1974. Landscapes of glacial erosion in Greenland and their relationship to ice, topographic and bedrock conditions. *Institute of British Geographers Special Publication,* 7**,** 177-195.

SUGDEN, D. & CLAPPERTON, C. 1981. An ice-shelf moraine, George VI Sound, Antarctica. *Annals of Glaciology,* 2**,** 135-141.

SUGDEN, D. E. & WATTS, S. 1977. Tors, felsenmeer, and glaciation in northern Cumberland Peninsula, Baffin Island. *Canadian Journal of Earth Sciences,* 14**,** 2817-2823.

SYRING, N., LLOYD, J. M., STEIN, R., FAHL, K., ROBERTS, D. H., CALLARD, L. & O'COFAIGH, C. 2020. Holocene interactions between glacier retreat, sea ice formation, and Atlantic water advection at the inner Northeast Greenland continental shelf. *Paleoceanography and Paleoclimatology,* 35**,** e2020PA004019.

WINKELMANN, D., JOKAT, W., JENSEN, L. & SCHENKE, H.-W. 2010. Submarine end moraines on the continental shelf off NE Greenland–Implications for Lateglacial dynamics. *Quaternary Science Reviews,* 29**,** 1069-1077.

XIE, S., DIXON, T. H., VOYTENKO, D., DENG, F. & HOLLAND, D. M. 2018. Grounding line migration through the calving season at Jakobshavn Isbræ, Greenland, observed with terrestrial radar interferometry. *The Cryosphere,* 12**,** 1387-1400.